Neurotoxicology 92 (2022) 33–48

Contents lists available at ScienceDirect

Neurotoxicology

journal homepage: www.elsevier.com/locate/neuro

Developmental neurotoxicity of acrylamide and its metabolite glycidamide in a human mixed culture of neurons and astrocytes undergoing differentiation in concentrations relevant for human exposure

Anna Jacobsen Lauvås [a,1], Malene Lislien [a,1], Jørn Andreas Holme [a], Hubert Dirven [a], Ragnhild Elisabeth Paulsen [b], Inger Margit Alm [a], Jill Mari Andersen [a], Ellen Skarpen [c], Vigdis Sørensen [c], Peter Macko [d], Francesca Pistollato [d], Nur Duale [a], Oddvar Myhre [a,*]

[a] Department of Chemical Toxicology, Norwegian Institute of Public Health (NIPH), Oslo, Norway
[b] Section for Pharmacology and Pharmaceutical Biosciences, Department of Pharmacy, University of Oslo, Norway
[c] Core Facility for Advanced Light Microscopy, Institute for Cancer Research, Oslo University Hospital, Oslo, Norway
[d] European Commission, Joint Research Centre (JRC), Ispra, Italy

ARTICLE INFO

Edited by Joao Batista Teixeira da Rocha

Keywords:
Acrylamide
Brain derived neurotrophic factor
Developmental neurotoxicity
Glycidamide
Human neural stem cells
Synaptogenesis

ABSTRACT

Neural stem cells (NSCs) derived from human induced pluripotent stem cells were used to investigate effects of exposure to the food contaminant acrylamide (AA) and its main metabolite glycidamide (GA) on key neurodevelopmental processes. Diet is an important source of human AA exposure for pregnant women, and AA is known to pass the placenta and the newborn may also be exposed through breast feeding after birth. The NSCs were exposed to AA and GA (1×10^{-8} – 3×10^{-3} M) under 7 days of proliferation and up to 28 days of differentiation towards a mixed culture of neurons and astrocytes. Effects on cell viability was measured using Alamar Blue™ cell viability assay, alterations in gene expression were assessed using real time PCR and RNA sequencing, and protein levels were quantified using immunocytochemistry and high content imaging. Effects of AA and GA on neurodevelopmental processes were evaluated using endpoints linked to common key events identified in the existing developmental neurotoxicity adverse outcome pathways (AOPs). Our results suggest that AA and GA at low concentrations (1×10^{-7} - 1×10^{-8} M) increased cell viability and markers of proliferation both in proliferating NSCs (7 days) and in maturing neurons after 14–28 days of differentiation. IC_{50} for cell death of AA and GA was 5.2×10^{-3} M and 5.8×10^{-4} M, respectively, showing about ten times higher potency for GA. Increased expression of brain derived neurotrophic factor (BDNF) concomitant with decreased synaptogenesis were observed for GA exposure (10^{-7} M) only at later differentiation stages, and an increased number of astrocytes (up to 3-fold) at 14 and 21 days of differentiation. Also, AA exposure gave tendency towards decreased differentiation (increased percent Nestin positive cells). After 28 days, neurite branch points and number of neurites per neuron measured by microtubule-associated protein 2 (Map2) staining decreased, while the same neurite features measured by βIII-Tubulin increased, indicating perturbation of neuronal differentiation and maturation.

1. Introduction

Acrylamide (AA) is a water-soluble substituted alkene that has been produced at a large scale for many years (Ghanayem et al., 2005; Hagmar et al., 2001), e.g. as an intermediate and as a monomer to produce polyacrylamide which can contain traces of AA monomers (EFSA, 2015; JECFA, 2005). Furthermore, AA is used in cosmetics and to produce textiles, in analytical biochemistry, and as soil conditioner for wastewater treatment (Friedman, 2003; Smith and Oehme, 1991; Tilson, 1981). The AA monomer is neurotoxic, reported to affect both the peripheral and the central nervous system (Erkekoglu and Baydar, 2014), and is classified as a probable human carcinogen (IARC, 1994). Therefore, concerns about exposure to AA of the general population arose with the discovery that AA was formed in carbohydrate-rich foods when

* Correspondence to: Norwegian Institute of Public Health, Department of Chemical Toxicology, Lovisenberggata 8, 0456 Oslo, Norway.
E-mail address: oddvar.myhre@fhi.no (O. Myhre).
[1] Equally contributing authors.

https://doi.org/10.1016/j.neuro.2022.07.001
Received 18 April 2022; Received in revised form 29 June 2022; Accepted 8 July 2022
Available online 11 July 2022

prepared at temperatures mostly above 120 °C and low moisture (Tareke et al., 2002).

AA-induced cumulative neurotoxic adverse effects have been well documented in occupational studies (Kütting et al., 2009). Workers are predominantly exposed via the respiratory tract and absorption through the skin (Bušová et al., 2020). AA is also absorbed by the oral route, as diet is an important source of human exposure (Dearfield et al., 1988; Duarte-Salles et al., 2013; Kleinjans et al., 2015; Pedersen et al., 2012; Sumner et al., 2003). Due to its high aqueous solubility, it is distributed into most tissues including the brain (Kim et al., 2015). In mammals including humans, AA is metabolized to the epoxide glycidamide (GA) by cytochrome P450 enzyme CYP2E1 (Kraus et al., 2013; Settels et al., 2008). GA can also be present in food items, but at lower concentrations than AA (Granvogl et al., 2008). It is currently unclear to which degree AA-induced neurotoxicity during fetal development is caused by the parent compound or its metabolite.

Results from the NewGeneris project showed that AA from dietary exposure readily crosses the placental barrier (Kleinjans et al., 2015; Pabst et al., 2005) and administration of ^{14}C-AA in pregnant mice resulted in distribution into the fetal brain (Marlowe et al., 1986). The concentrations of AA and GA in fetal circulation and maternal blood are approximately in the same range (Annola et al., 2008; Pedersen et al., 2012; von Stedingk et al., 2011), indicating that the placenta barrier only provides a limited protection. Following birth, the child may be exposed to AA and GA via breast milk (Sörgel et al., 2002). Embryonic, fetal and childhood periods contain neurodevelopmental stages (windows) that are highly sensitive to chemical exposure (Andersen et al., 2000; Grandjean and Landrigan, 2006).

Normal human brain development is a complex process with both time-dependent and spatial patterning, and concern has been expressed over the impact of toxicants on brain development during pregnancy (Hessel et al., 2018). Brain development involves processes including neuronal proliferation, commitment of neuronal and glial progenitor cells, migration, differentiation into neuronal and glial cells, synaptogenesis, pruning, myelination, network formation and functional neuronal and glial cell maturation (Hessel et al., 2018; Hogberg et al., 2010, 2009; Kang et al., 2011; Krug et al., 2013; Rice and Barone, 2000; Silbereis et al., 2016; Stiles and Jernigan, 2010). Many of these neurodevelopmental processes identified in vivo can now be mimicked using neural stem cell (NSC) models (Davidsen et al., 2021; Di Consiglio et al., 2020; Fritsche et al., 2018, 2021; Pistollato et al., 2017a, 2021, 2020, 2014; Sachana et al., 2018).

Numerous studies have reported neurotoxicity of AA in adult animals (as reviewed by e.g. (EFSA, 2015)). Less is known regarding its effects on early pre- and postnatal neurodevelopment. Previous animal studies show developmental neurotoxicity (DNT) after pre- and perinatal exposure to AA, including disturbed auditory startle response and neurobehavioral effects (Ferguson et al., 2010; Garey and Paule, 2007, 2010; Krishna et al., 2015; Krishna and Muralidhara, 2018; Wise et al., 1995), brain weight loss and brain development (Allam et al., 2011; Dortaj et al., 2018; El-Sayyad et al., 2011; Lai et al., 2017; Ogawa et al., 2011, 2012), effects on biomarkers linked to mitochondrial dysfunction (El-Sayyad et al., 2011; Krishna et al., 2015) and oxidative stress (Allam et al., 2013, 2011; El-Sayyad et al., 2011; Erdemli et al., 2018, 2016; Krishna et al., 2015; Krishna and Muralidhara, 2018; Lai et al., 2017; Ogawa et al., 2011). Studies in various cell models undergoing differentiation report effects linked to DNT, such as reduced neurite outgrowth (Attoff et al., 2016; Chen and Chou, 2015; Chen et al., 2014; Lee et al., 2018; Radad et al., 2019), disturbed proliferation and differentiation (Attoff et al., 2017, 2020, 2016; Chen and Chou, 2015; Chen et al., 2014; Park et al., 2010) as well as more general toxic effects including mitochondrial dysfunction (Lee et al., 2018) and oxidative stress (Park et al., 2010). In the animal studies, the concentrations used were far above relevant exposure for pregnant women (reviewed by (EFSA, 2015; Lindeman et al., 2021)). Furthermore, only a couple of studies have used human induced pluripotent stem cell (iPSCs)-derived NSCs (Kobolak et al., 2020; Schmuck et al., 2017), and none have compared AA and GA. HiPSC-derived NSCs and their differentiated derivatives, combined with other new approach methods such as computational and mathematical models, along with refinement approaches (e.g., use of zebrafish eleutheroembryos) are currently considered relevant for DNT testing (Bal-Price et al., 2018b). Over the recent years, activities have been initiated within the Organisation for Economic Co-operation and Development (OECD) and The European Food Safety Authority (EFSA), addressing the need for implementation of faster, more cost efficient and human relevant methods compared to current animal guideline studies. In this context, a guidance document is currently being prepared with the purpose to instruct on the regulatory use of a developmental neurotoxicity in vitro testing battery with fit-for-purpose applications (Crofton and Mundy, 2021; Sachana et al., 2021).

Altogether, there is a need for performing studies comparing the toxicity of AA and GA at real-life concentrations and in human relevant NSC models. The main aim of this study was to investigate whether exposure of AA and GA close to levels found in human blood affects key neurodevelopmental processes considered to be vital for normal brain development. This was achieved through an in vitro approach using human NSCs derived from hiPSC exposed to AA and GA for up to 28 days of differentiation. The NSC model was characterized to show feasibility for neurodevelopmental studies of toxicants such as AA and GA, with the purpose to identify molecular targets and endpoint anchored to key events identified in the existing DNT adverse outcome pathways (AOPs).

2. Materials and methods

2.1. Human iPSC culture, NSC expansion, differentiation and treatment with acrylamide and glycidamide

The IMR90-hiPSC-derived neural stem cells (NSCs) were kindly provided by Dr. Anna Bal-Price (European Commission, Joint Research Centre, Ispra, Italy). The IMR90-hiPSC were previously obtained by reprogramming IMR90 fibroblasts by viral transduction of Oct4 and Sox2 genes using pMIG vectors (addgene) at I-Stem, Paris, France. Rosette-derived NSCs had previously been obtained by Dr. Francesca Pistollato at the JRC as described in (Pistollato et al., 2017b; Zagoura et al., 2017).

NSCs were thawed from a cryopreserved state and cultivated in Neural Induction Medium (DMEM/F12 GlutaMAX, with non-essential amino acids, N2-and B27-supplements without Vitamin A, 50 U/mL Penicillin/Streptomycin, 2 μg/mL Heparin grade I-A (sigma Aldrich), 10 ng/mL basic fibroblast growth factor (bFGF), 10 ng/mL epidermal growth factor (EGF) and 2.5 ng/mL brain derived neurotrophic factor (BDNF), from Thermo Fischer), refreshing medium three times a week. NSCs were passaged by enzymatic dissociation with 0.05% Trypsin-EDTA and replated at a density of 13.300 cells/cm^2 in flasks pre-coated with Matrigel Basement Membrane Matrix (1:100 in DMEM/F12 GlutaMAX, Corning). NSCs to undergo differentiation were replated in 96-well plates pre-coated with poly-D-lysine and Growth Factor Reduced Matrigel (1:100 in DMEM/F12 GlutaMax, Corning) at a density of 21.000 cells/cm^2 in Neural Induction Medium. NSCs were differentiated for 28 days into a mixed culture of neurons and astrocytes in the presence of Neural Differentiation Medium (Neurobasal medium, N2- and B27-supplements, 2 mL L-Glutamine, 50 U/mL Penicillin/Streptomycin, 2.5 ng/mL BDNF, 1 ng/mL glial cell line-derived neurotrophic factor (GDNF) and 1 μg/mL Laminin, all from Thermo Fischer), refreshing medium twice a week.

2.2. Assessment of cytotoxicity with Alamar Blue™ cell viability assay

Cells were plated in 96-well plates with a density of 21.000 cells/cm^2 in Neural Induction Medium. Stock solutions of AA, GA and 1:1 combination of these were dissolved in water and sterile filtered using a 0.22

μm pore filter (Merck Millipore Ltd., Co. Cork, Irland) and syringe (Becton Dickinson S.A., Madrid, Spain). Dilution series of AA, GA and the combination of (AA + GA) were then created in Neural Differentiation Medium, reaching final, total concentrations in the range of 3×10^{-3} M - 3×10^{-8} M. The cells were exposed to the chemicals with 6 internal replicates per concentration, and chemical-containing medium was refreshed twice a week. Sterile water (0.1%) was added to vehicle control cells in a similar ratio as exposed cells. At 24 h (1 day), 72 h (3 days) and 14 days of differentiation in vitro, cells were incubated in Neural Differentiation Medium containing 10% resazurin (Invitrogen, DAL1100) for 3 h and 30 min at 37 °C, 5% CO_2. Resazurin is the active ingredient in the Alamar Blue™ cell viability assay, and upon contact with viable cells is reduced to resorufin, which is more fluorescent than resazurin. After incubation, fluorescence was read at excitation/emission 560/590 nm with CLARIOstar® microplate reader (BMG Labtech, Ortenberg, BW, Germany). At least 3 independent experiments were performed (i.e., average of at least 3 cell passages).

2.3. Gene expression analysis

Total RNA from four independent experiments (cell passages) from unexposed cells undergoing differentiation for 0, 3, 7, 14, 21 or 28 days were isolated using Qiagen RNeasy Micro kit (Qiagen, Hilden, Germany) according to the manufacturer's protocols. The isolated RNA quantity and integrity were assessed as previously described (Duale et al., 2014; Aarem et al., 2016) using a NanoDrop 1000 Spectrophotometer (Thermo Scientific, Massachusetts, USA) and Agilent 2100 Bioanalyzer (Agilent Technologies, Santa Clara, California, USA) with an RNA integrity number (RIN) acceptance criteria over 7.0, and RNA from all samples had an average RIN over 9. All samples were stored at – 80 °C prior to gene expression analysis.

For RNA sequencing analysis, cDNA library construction was performed from the isolated total RNA (500 ng, quantified by Qubit 2.0 fluorometer) using the QuantSeq 3′mRNA-Seq Library Prep FWD kit (Lexogen, Vienna, Austria) according to the manufacturer's protocols. The libraries were QC (quality control) checked for cDNA size and distribution using the Agilent 4200 TapeStation system (Santa Clara, California, USA). Multiplexed single-read sequencing (1 ×75 bp) was performed on an Illumina® NextSeq 550 platform (Illumina®, San Diego, CA, USA). Raw reads fastq-files were trimmed using TrimGalore (Version 0.6.5) and trimmed reads were mapped to the human genome (version GRCh38) using HISAT2 (version 2.2.0.) (Kim et al., 2019). Counting of mapped reads was done using featureCounts v1.6.2 (Liao et al., 2014) based on annotation from Ensembl release 84. Between 13 and 16 million reads were generated per library and the overall mapping rate was between 85% and 90%. The raw gene counts were normalized for inherent systematic or experimental biases (e.g., sequencing depth, gene length, GC content bias etc.). Prior to the statistical testing procedure, the raw gene read counts were further preprocessed, i.e., filtering out feature with zero read counts in all samples before statistical analyses. The resulting filtered raw gene counts were then normalized and used for differential expression testing using DESeq2 (Love et al., 2014). The following contrasts: 3 days of differentiation versus day 14, day 3 versus day 21, and day 14 versus day 21 were compared. The genes with log2-Fold change $> \pm 1.0$ and adjusted p-value < 0.05 were considered as differentially expressed genes (DEG) (upregulated or downregulated genes).

For qPCR analysis, the reverse transcription reaction and real-time qPCR were carried out as previously described (Duale et al., 2014, 2010). In brief, total RNA (1000 ng) from at least three independent experiments of unexposed cells undergoing differentiation for 0, 3, 7, 14, 21 or 28 days was reverse transcribed to cDNA using the High-Capacity cDNA Reverse Transcription Kit (Thermo Fischer, Massachusetts, USA) according to the manufacturer's protocol. The resulting reverse transcription reaction product was stored at − 20 °C for further analysis. cDNA was diluted 1:50 and qPCR reactions were run in triplicates using TaqMan Gene Expression Master mix and TaqMan Gene Expression Assays (all Thermo Fischer, see Supplementary Table 1) with an annealing temperature of 60 °C, as recommended by the manufacturer's protocol on a CFX384 Touch Real-Time PCR Detection System (Bio-Rad, Hercules, California, USA). For the data analysis, only the mean Cq of at least two technical replicates with a technical variation of SD < 0.3 were accepted. Missing values and Cq > 40 were replaced by an established limit of detection of Cq $= 41$ and the gene expression levels were calculated with the ΔΔCq method (Livak and Schmittgen, 2001; Schmittgen and Livak, 2008) as previously described (Duale et al., 2012, 2010).

2.3.1. Enrichment analysis

Identification of the enriched biological processes and pathways was carried out using Metascape (http://metascape.org/) (Zhou et al., 2019). Metascape is a powerful annotation analysis tool for gene function, and it integrates several functional databases such as GO, KEGG, and Uniprot to analyze not only a single data set, but also multiple gene-sets simultaneously. The Matascape was used to identify enriched functional pathways of the statistically differentially expressed genes for RNAseq analysis.

2.4. Protein expression of neural differentiation markers

2.4.1. Experimental design and immunostaining

Two separate experiments were performed. In the first experiment, cells were plated in Neural Induction Medium at a density of 21.000 cells/cm^2 in 96 well plates pre-coated with Poly D-Lysine and Growth Factor Reduced Matrigel. After 24 h, the medium was changed to Neural Induction Medium containing 10^{-4} and 10^{-7} M AA or GA. The test concentrations were selected partly based on the observed increase in cell viability, and on human blood levels (see Section 4.1 for further details). Medium and chemicals were refreshed three times during the 7 days exposure. Vehicle control cells were maintained in Neural Induction Medium containing 0.1% sterile water.

The second experiment followed a similar experimental setup as experiment 1, plating 21.000 cells/cm^2 in Neural Induction Medium in poly-D-lysine precoated 96-well plates. After 24 h, the cells underwent a complete medium change to Neural Differentiation Medium containing10^{-4} and 10^{-7} M AA or GA, or 0.1% sterile water (vehicle control). The medium with chemicals was prepared fresh and changed twice a week.

After 7 days of proliferation and exposure (Experiment 1) and 7, 14, 21 and 28 days of combined exposure and differentiation (Experiment 2), the cells were fixed for 10 min with 4% paraformaldehyde (252,549–100 mL, Sigma) and washed twice in PBS with Mg^{2+} and Ca^{2+}. The cells were then permeabilized in 0.1% Triton™ X-100 solution (93,443–100 mL, Sigma Aldrich) in 3.5% BSA (A7979–50 mL, Sigma-Aldrich) for 15 min at room temperature and blocked for 15 min in 3.5% BSA. After washing with PBS with Mg^{2+} and Ca^{2+}, the cells were incubated with primary antibodies in batches and dilutions as seen in Table overnight at 4 °C. The next day, the primary antibody solutions

Table 1
Primary antibodies and dilutions.

Batch	Primary antibody	Dilution	Catalog number	Company
1	Nestin	1:400	N5413–100UG	Sigma-Aldrich
	Ki67	1:400	MAB4190	Sigma-Aldrich
	GFAP	1:300	PA1–10004	Thermo Fischer
2	BDNF	1:1000	OSB00017W	Thermo Fischer
	ßIII-Tubulin	1:1000	801202	BioLegend
	GFAP	1:300	PA1–10004	Thermo Fischer
3	MAP2	1:5000	Ab5392	AbCam
	Syp	1:1:200	Ab14692	AbCam
	PSD95	1:1:300	Ab13552	AbCam

were recovered, and the cells were incubated with secondary antibodies as shown in Tables 1 and 2 for 1 h in darkness. The cells were then washed twice and stored in PBS with Mg^{2+} and Ca^{2+} until fluorescence microscopy. Both experiment 1 and 2 were repeated in four independent experiments (cell passages) with four internal replicates (wells) for each immunostaining.

2.4.2. Fluorescence microscopy and high content imaging

Immunostained cells were imaged on a Nikon ECLIPSE Ti2-E microscope (Nikon Corp, Tokyo, Japan) using a CFI S Plan Fluor LWD 20XC (NA 0.7) objective, a CSU-W1 spinning disk confocal unit (50 μm pinhole size, Yokogawa Electric Corp, Tokyo, Japan), a Prime BSI sCMOS camera (Teledyne Photometrics, Tucson, AZ, US), 405 nm, 488 nm, 561 nm and 638 nm lasers, BrightLine bandpass filters (447/60, /525/50, 600/52, and 708/75), and NIS-Elements AR 5.30 software. Multichannel images (DAPI, GFP, RFP, and AF647 channels) of 6 random fields of view in each well were captured. For each field of view, 5 optical Z-sections were acquired with Z-section spacing 1 μm. Z-sections were projected by the maximum intensity projection method, and all images were converted into tiff using NIS-Elements AR Analysis software.

Mean fluorescence intensity and the relative percentages of immunostained cells were quantified using the CellInsight™ CX7 High Content Analysis Platform (Thermo Fisher) and the ArrayScan Neuronal Profiling V4.2 and Compartmental Analysis V4 BioApplications. Through these algorithms, live DAPI+ nuclei are identified by a specific nucleus mask, and the cell type antibody/antigen staining (i.e., Map2, β-III-Tubulin, GFAP or Nestin) is identified by a cell body mask. Neuronal Profiling V4.2 BioApplication enables the measurement of neurite outgrowth features, measuring the number of neurites per neuron, the length of the neurites (expressed in μm) and the number of branch points per neurite (neurite branching) as described in (Davidsen et al., 2021). BDNF fluorescence intensity levels and synapses, identified by co-localization of SYP and PSD95 puncta, were quantified using the same bioapplication and following a Thermo-Fisher standardized protocol (ThermoFisherScientific, 2022). The data are presented as 3–4 independent experiments (i.e., average of 3–4 cell passages, with 4 technical replicates (wells) in each passage).

2.5. Statistical analysis

To compare differentiated cells to undifferentiated, or exposed to control cells, analysis of variance was performed by the Standard Least Squares method. Outliers in experimental groups were detected and removed by Grubbs test, with a significance level $\alpha = 0.05$. The p-values were adjusted by false detection rate and a post hoc test of Dunnet's comparisons to control/undifferentiated cells was performed. All statistical analysis was performed in JMP pro 16.1 (SAS institute, Cary, NC). For the RNAseq data, differentially expressed genes (DEGs) were identified using the DESeq2 R-package (Love et al., 2014). Statistical analysis was done using JMP Pro 16 (SAS institute, NC, USA) and R statistical software (Version 4.1.0., R Development Core Team, (RStatisticalProject, 2022)), with at least 3 independent experiments (i.e., average of 3 cell passages, with 4–6 technical replicates (wells) in each passage.

3. Results

Neural stem cells (NSCs) are characterized by a conical (triangular) shape, which is seen in Fig. 1A. Immature neurite network formation can be seen after 7 days (Fig. 1B), and a more mature morphology can be observed at 14–21 days of differentiation (Fig. 1C and D), when the cells aggregate and form more complex neurite networks. In order to quantify the neurite length, cells were stained with Map2. Immunostaining of NSCs undergoing differentiation revealed a maturing neuronal culture with increased neurite network formation after 21 and 28 days (Fig. 1E).

3.1. Differentiation of hiPSC-derived NSCs to a mixed culture of neurons and glia

3.1.1. Characterization of the model

To elucidate how the transcriptome of NSCs fluctuate during differentiation, the transcriptional profile of unexposed NSCs undergoing differentiation for 3, 14 and 21 days was performed by RNAseq analysis. The results from the RNAseq analysis revealed that there was a clear separation of the NSCs based on differentiation days (Fig. 2A and B). By visual inspection of the clustering dendrogram (Fig. 2A), we observed that samples from cells differentiated for 3 days seemed to cluster close to each other and shared a similar expression pattern, while samples from 14 and 21 days of differentiation cluster close to each other. A principal component analysis (PCA) revealed similarities and contrasts between the three differentiation periods (Fig. 2B). The PCA plot shows that the principal component 1 separates groups of the three differentiation periods (3, 14 and 21 days) into two separate clusters, i.e., samples from 3 days of differentiation cells in one cluster, while samples from 14 and 21 days in another cluster (Fig. 2B).

The next step was to identify genes where the transcription levels changed during the NSC differentiation, to further confirm previous characterization of the cell model (Davidsen et al., 2021; Di Consiglio et al., 2020; Pistollato et al., 2017a, 2014) and transferability between laboratories. We used DESeq2 R-package, which is designed for normalization, visualization, and differential analysis of high- dimensional count data to select genes whose mean expression level is significantly different between the three differentiation stages. Volcano plots of the comparisons are shown in Fig. 2 D-F. The number of genes that were differentially expressed (adjusted p-value < 0.05) between 3 and 14 days of differentiation was 1140 genes (621 overexpressed whereas 519 genes were downregulated). An extensive number of genes (3070 in total) were identified as differentially expressed between 3 and 21 days (1531 upregulated, 1539 downregulated). Further, 1070 genes were identified as differentially expressed between 14 and 21 days (511 upregulated, and 559 downregulated). A Venn diagram of the differentially expressed genes between the three contrasts are shown in Fig. 2C, and there were 306 shared genes between the three contrasts. Furthermore, some selected genes involved in neurodevelopment, metabolism or PI3/AKT/mTOR pathways an intracellular signaling pathway important in regulating the cell cycle, are presented in Fig. 2G-H.

To determine the biological relevance of the differentially expressed genes, we investigated their biological functions using Metascape (Zhou Y et al., 2019). The Metascape uses accumulative hypergeometric p-values and enrichment factors to select enriched terms within a gene set. This analysis aimed at understanding the effect of the modulation of

Table 2
Secondary antibodies and dilutions.

Secondary antibody	Dilution	Catalog number	Company
Goat Anti-Chicken IgY H&L DyLight® 488	1:500	ab96951	AbCam
Goat Anti-Mouse IgG H&L DyLight® 550	1:500	ab96902	AbCam
Goat Anti-Rabbit IgG H&L DyLight® 650	1:500	ab96880	AbCam
DAPI	1:1000	62248	Thermo Fischer

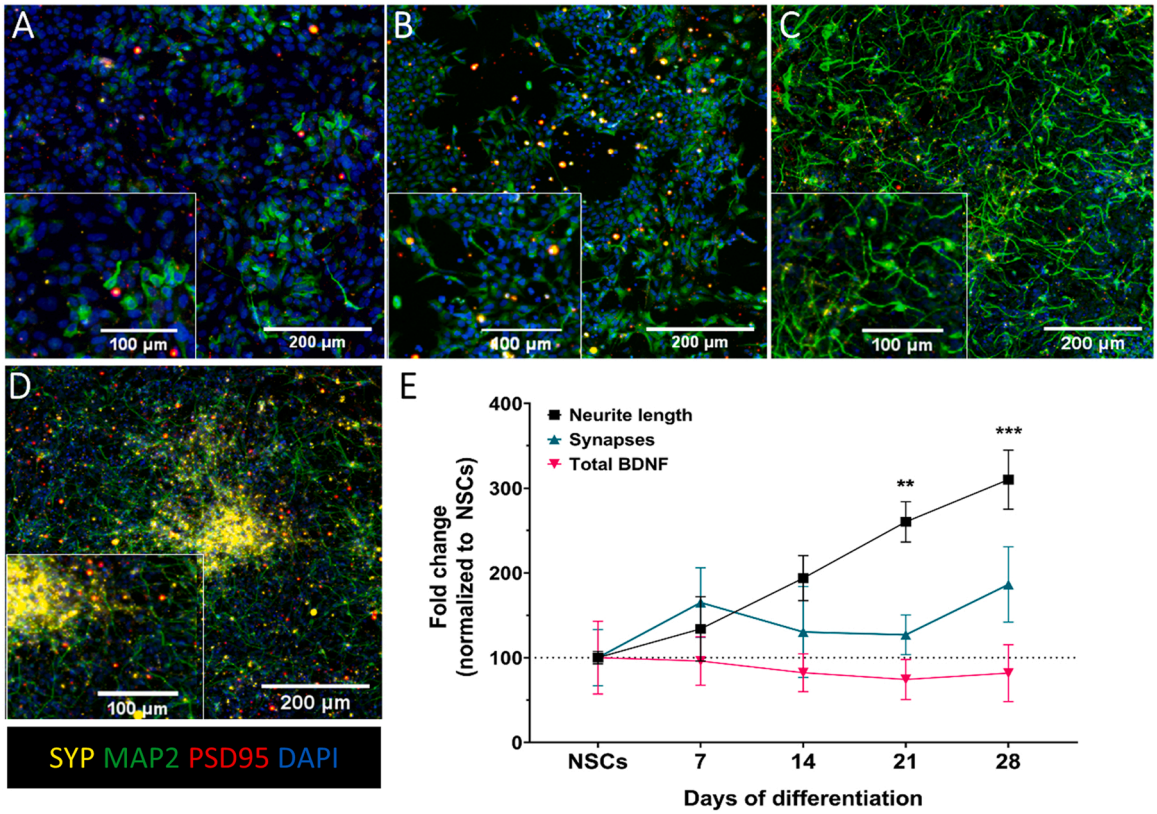

Fig. 1. Neural stem cells undergoing differentiation towards a mixed culture of neurons and astrocytes for 0 (A), 7 (B), 14 (C) and 21 (D) days. Nuclei are identified by DAPI (blue), neurons and neurites by Map2 (green) and synapses as overlap between PSD95 (red) and synaptophysin (yellow). Neurite length measured by Map2, number of synapses measured as puncta overlap of SYP and PSD95 and total BDNF levels in NSCs undergoing differentiation (E). The data are calibrated on NSCs and are presented as mean ± S.E.M. of 3–4 independent experiments (cell passages) (** = $p < 0.01$ and *** = $p < 0.001$, compared to NSCs).

gene expression on a particular cellular function. Metascape results represent a global picture of biological processes, molecular functions and cellular co-localizations that are significantly enriched following neuronal differentiation. The top 20 clusters for the identified differentially expressed gene list with their representative enriched terms are presented in Fig. 3A and B, and process enrichment analysis were performed with the KEGG pathway, GO biological processes, Reactome gene sets, canonical pathways, and CORUM. The most significantly enriched terms among over-expressed genes during NSCs differentiation include genes related to neurodevelopment in general such as neural nucleus development, regulation of neurogenesis, gliogenesis, sensory organ and brain development (Fig. 3A), while genes involved in cell cycle, mitotic cell cycle, DNA metabolic process, DNA double-stand break repair, chromosomal organization or microtubule cytoskeleton organization were enriched in the under-expressed gene list (Fig. 3B).

The expression levels of selected genes in NSCs undergoing differentiation towards a mixed culture of neurons and astrocytes are shown in Fig. 4A and B. The expression level of *NES*, a marker of NSCs, showed no significant change in differentiated cells compared to NSCs (Fig. 4A). The expression level of *GAP43*, which is involved in growth cone motility and axonal outgrowth (Chung et al., 2020), was significantly increased by 5-fold and 3-fold at 21 and 28 days of differentiation compared to the undifferentiated cells, respectively. The expression of *MAP2* and *MAPT* genes were analyzed to confirm the maturation of NSCs into committed neurons. Indeed, differentiation time dependent increase in the *MAP2* gene expression level was observed, with a peak of 2-fold increase at 28 days. A similar gene expression pattern for *MAPT* and *SYP* genes were observed with an approximately 6-fold and 5-fold increase at 21 and 28 days, respectively. The simultaneously increased expression of *SLC1A2* gene (encoding a glutamatergic transporter) indicated the presence of a mixed culture of post-mitotic neurons and glial cells at 21 and 28 days of differentiation. To elucidate whether the neuronal cell culture was of an excitatory or inhibitory type, the expression levels of *GABRA3*, *GRIN1*, *NR4A2* and *SLC32A1* genes were investigated. As shown in Fig. 4B, the expression level of *GABRA3* gene was significantly increased by 5-fold at 21 days of differentiation. The observed increase in expression level of *GRIN1* and *SLC32A1* genes at 21 and 28 days and *NR4A2* at 21 days, indicated the presence of an inhibitory/excitatory neuronal culture consisting of both GABAergic, glutamatergic, and dopaminergic neurons.

3.2. Exposure to acrylamide and its metabolite glycidamide and effects on neuronal differentiation

3.2.1. Part 1: assessment of cytotoxic concentrations and potency

A 1-day, acute exposure of NSCs to low concentrations of AA, GA and a 1:1 mixture of these resulted in an increased mitochondrial activity as measured by the Alamar Blue™ cell viability assay of approximately 15–25% in the concentration range 3×10^{-7} to 10^{-3} M (AA) and 3×10^{-7} to 3×10^{-4} M (GA and mixture) (Fig. 5A, B and C). The increase in mitochondrial activity was somewhat higher (5–10%) in cells exposed to AA and the 1:1 mixture than GA. After 14 days of repeated exposure to the same concentration range during differentiation towards a mixed culture of neurons and astrocytes, continued exposure to low concentrations of each treatment resulted in an increased mitochondrial activity of 5–10% and 10–15% to cells exposed to AA and GA, respectively. No increased viability was observed in cells exposed to the mixture after 14 days. Complete cell death was observed in cells exposed to 10^{-3} and 3×10^{-3} M of AA and the mixture, whereas complete cell death was observed after exposure to 3×10^{-4} M to 3×10^{-3} M of GA. The relative differences seen on mitochondrial activity between AA and GA at low concentrations and in their relative potency to induce cell

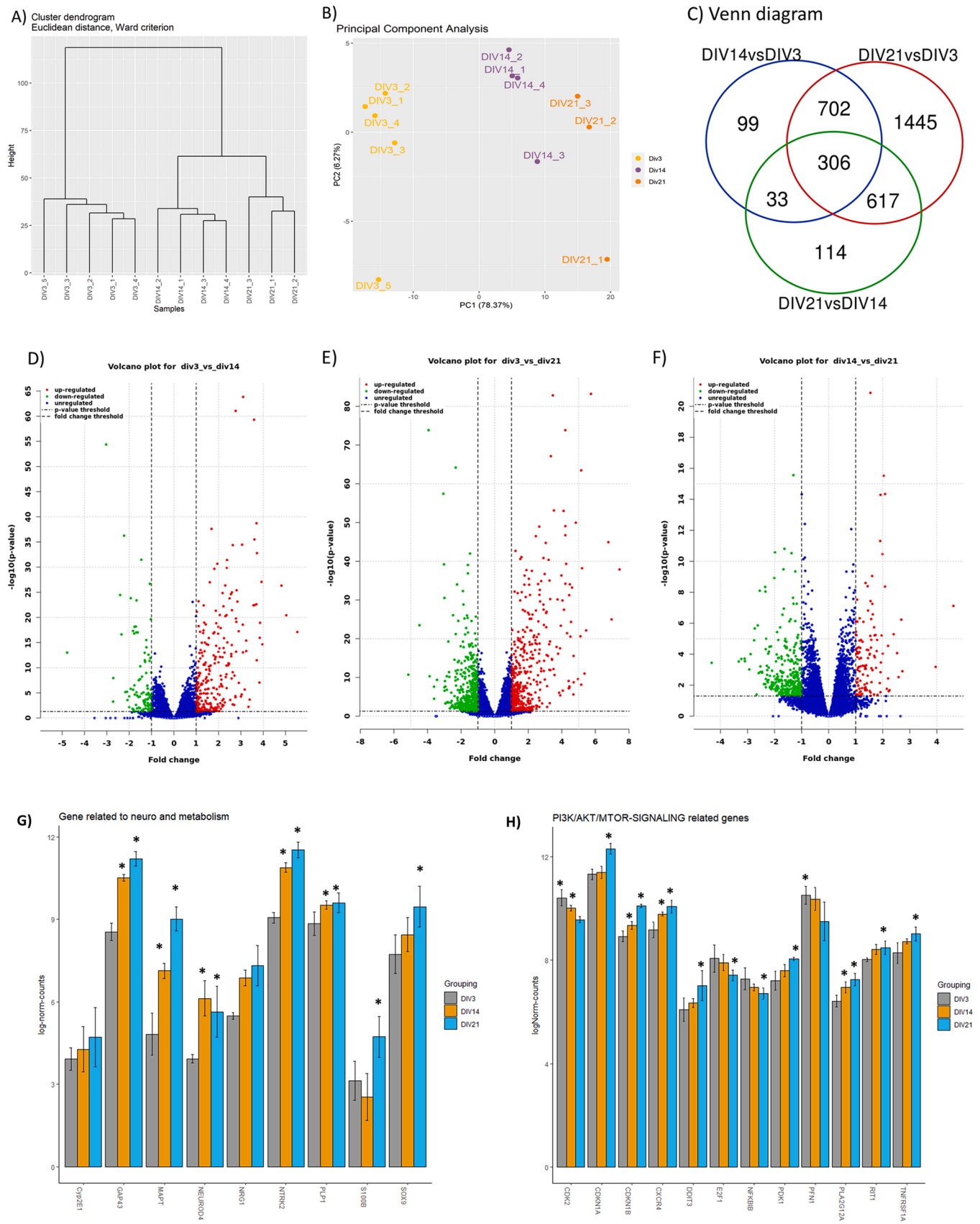

Fig. 2. Transcriptomics analysis of differentiating NSC. A) Clustering dendrogram of NSC samples. B) Principal component analysis of NSC samples. C) Venn diagram of differentially expressed genes between differentiation days 3, 14 and 21 (legends DIV3, DIV14 and DIV21). D-F) Volcano plot of the different comparisons. G-H) The expression level of some selected genes involved in the PI3K/AKT/MTOR-signaling pathway and neurodevelopment/metabolism related genes. Bar-plots (G-H) are presented as mean ± S.E.M. of 3–4 independent experiments (* = adjusted $p < 0.05$ compared to DIV3).

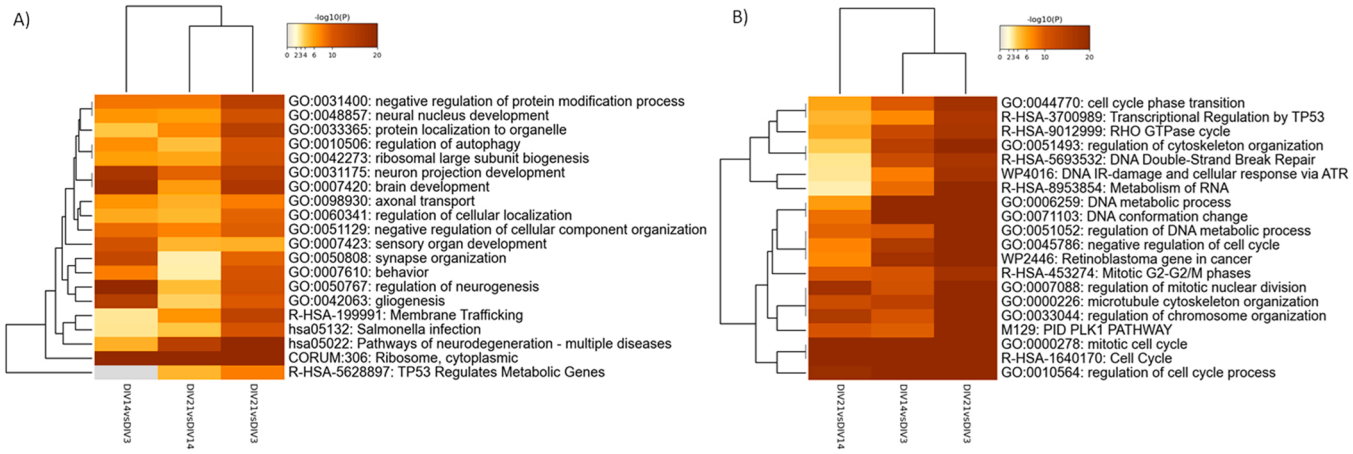

Fig. 3. Functional enrichment analysis of differentially expressed genes between differentiation days 3, 14 and 21. A) Heatmap of enriched Go-terms or pathway for the significantly upregulated genes, B) Heatmap of enriched Go-terms or pathway for the significantly downregulated genes. In total 3–4 independent experiments (cell passages) were performed.

death at high concentrations, made us hypothesize GA was more potent than AA. To investigate this, we exposed NSCs to a more extensive concentration range of AA and GA for 3 days. After 3 days of differentiation, increased mitochondrial activity in cells exposed to 10^{-7} and 3×10^{-7} M of both AA and GA was observed (Fig. 6). IC_{50} was determined by 4-parameter logistical regression to be 5.2×10^{-3} M (95% CI: [4.2×10^{-3} M, 6.5×10^{-3} M]) and 5.8×10^{-4} M (95% CI: [5.1×10^{-4} M, 6.5×10^{-4} M]) for AA and GA, respectively, indicating GA to be about 10 times more potent to induce cytotoxicity in NSCs undergoing differentiation than AA.

3.2.2. Part 2: assessment of protein levels and morphological changes by high content imaging

7 days of exposure to 10^{-7} M GA during proliferation caused a two-fold increase in Nestin+ cells and cells expressing the proliferation marker Ki67, and a three-fold increase in cells co-expressing Nestin and Ki67, compared to vehicle control cells. AA caused no significant change in any of the proliferation markers (Fig. 7A-E).

When exposing NSCs undergoing differentiation for 7–28 days to 10^{-7} and 10^{-4} M AA or GA, no significant changes in synapse numbers (measured by puncta overlap between PSD95 and SYP) and total BDNF levels could be observed upon AA exposure at any time points (Fig. 8 B-E)). Notably, exposure to 10^{-7} M GA for 7–28 days during differentiation (Fig. 8 A) showed a significant decrease of 20–40% in synapses after 21 and 28 days in differentiation (Fig. 8D and E). At the same time points, an increase in total levels of BDNF could be observed upon exposure to 10^{-7} M GA (Fig. 8D, E). Moreover, exposure to 10^{-7} M GA during differentiation caused an increase in % glial fibrillary acidic protein positive (GFAP+) cells by approximately 200% and 50% after 14 and 21 days, respectively (Fig. 9A, B). The same treatment caused an increase of approximately 50–80% of cells expressing Ki67, after 14 and 28 days (Fig. 9A, C), and a steady increase in the cell population expressing Nestin after 14, 21 and 28 days (Fig. 9A–C).

The increase of %Nestin+ cells, %GFAP+ cells and cells expressing Ki67 indicate a slightly immature environment when it comes to differentiation towards a culture of committed neurons. These results made us hypothesize that markers of neuronal differentiation towards committed neurons after treatment with 10^{-7} M GA would decrease and markers of immature neurons would increase. To investigate this, we quantified the %neurons and features relevant for neuronal network formation in the cell culture by two neuronal markers. ßIII-Tubulin was chosen as a marker for quantification of immature neurons and neurites and Map2, marker of dendrites, was chosen as a marker for more committed and fully developed neurons and neurites. Arborization measured by quantification of branch points in ßIII-Tubulin+ neurites (Fig. 10B) showed an increase of approximately 25% after both 21 and 28 days of treatment with 10^{-7} GA during differentiation. At 28 days, neurite length quantified by Map2 expression (Fig. 10B) increased by 20% compared to vehicle control. Although no significant change was observed in the percentage of committed neurons quantified by Map2 after 21 days, the number of Map2 + neurites per neuron (Fig. 10 D) was significantly reduced by 10%.

4. Discussion

Our study provides new insights about the biological plausibility between developmental exposure to AA and in particular GA at human relevant concentrations (10^{-7} M) and disturbance of neurodevelopmental processes (i.e., neuronal cell injury and cell death, disturbed proliferation, neuronal maturation, neurite outgrowth, synaptogenesis, increased brain derived neurotrophic factor (BDNF) level and gliogenesis) vital for normal brain development. The lack of effects on these neurodevelopmental differentiation processes at higher AA and GA concentrations (10^{-4} M) indicate a biphasic response curve. A biphasic response curve may suggest that AA and GA trigger both inhibitory as well as stimulatory signals for the neurodevelopmental differentiation processes, where the outcome depends on the concentration. However. these speculations of lack of effects at higher and less relevant concentrations need further verifications, thus below we only discuss our results obtained in the lower concentration range.

Characterization of the cell culture during differentiation from day 3–21 showed differentially expressed genes (DEGs) and protein markers for neurodevelopmental processes (including synaptogenesis, gliogenesis, neurite outgrowth, BDNF, neuronal and glia commitment and maturation) in addition to metabolic competence (including Cyp2E1) in line with previous publications on the same NSC model using similar differentiation protocols (Davidsen et al., 2021; Di Consiglio et al., 2020; Pistollato et al., 2017b, 2021, 2014). Also, increasing levels of e.g. *GAP43* and *MAPT* under differentiation shown by the RNAseq analysis are in line with the qPCR results. Clearly, the cluster dendrogram shows that the different cell passages at each day of differentiation (3, 14, 21 days) were quite similar, and that the number of DEGs were largest between 3 and 21 days of differentiation, compared to day 3 versus day 14, and day 14 versus day 21. Interestingly, functional enrichment analysis showed that most of the upregulated genes were enriched in neurodevelopment related terms, while most of downregulated genes were enriched in cell cycle related terms. For example, selected analysis showed DEGs of the PDK1/Erk/Akt/mTOR pathway after 3, 14 and 21 days of differentiation. mTOR regulates neurodevelopmental processes such as proliferation, differentiation, migration, and dendrite formation,

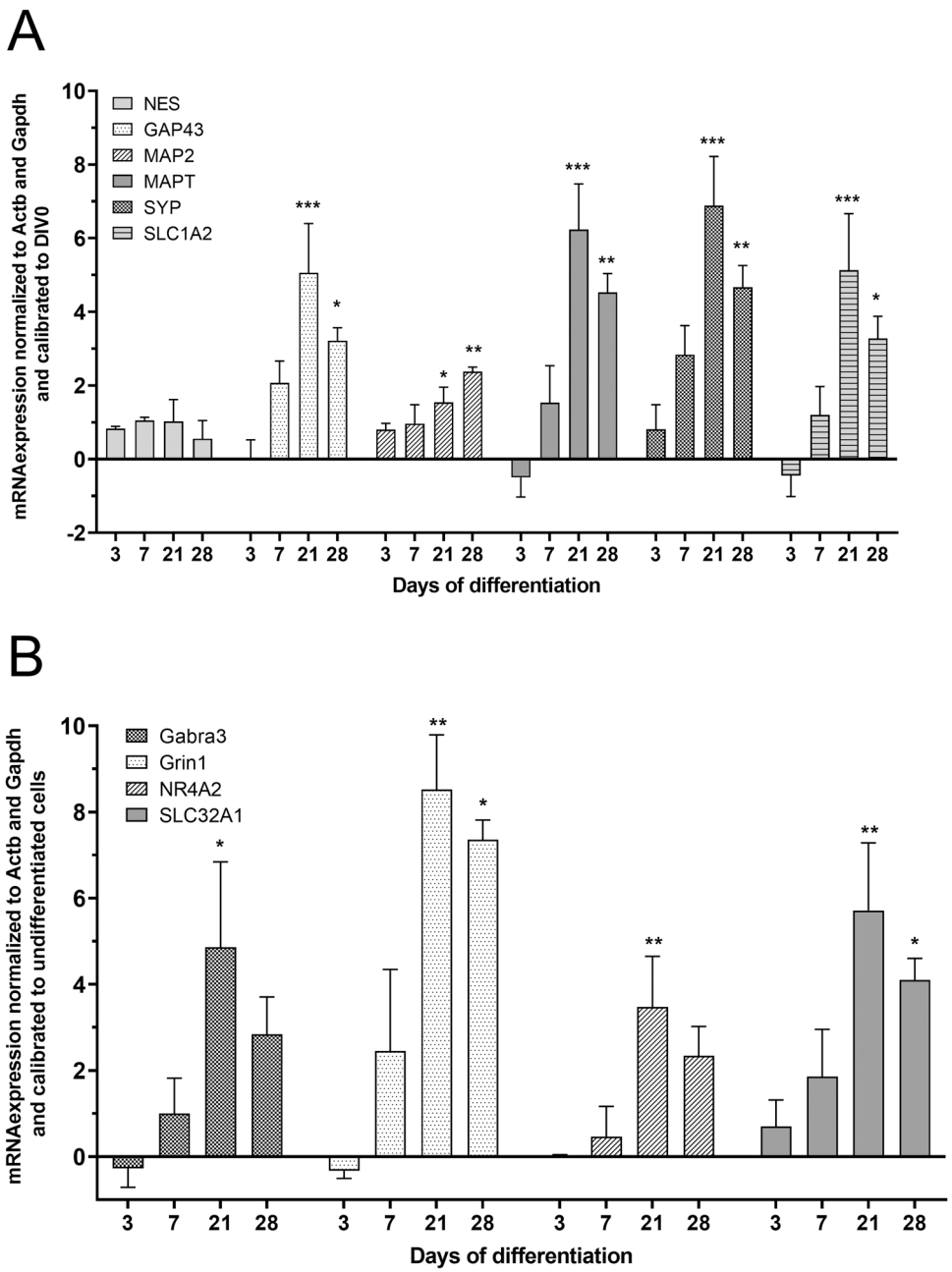

Fig. 4. mRNA in neural stem cells undergoing differentiation towards a mixed culture of neurons and astrocytes. A) Markers of neuronal and glial differentiation and B) markers of neuronal subtypes of glutamatergic, GABAergic and dopaminergic neurons. The data are calibrated on undifferentiated cells and are presented as mean ΔΔ Ct ± S.E.M. of at least 4 independent experiments (cell passages) (* = $p < 0.05$, **= $p < 0.01$ and *** = $p < 0.001$, compared to NSCs).

and is furthermore central in synaptic formation and plasticity (reviewed in (LiCausi and Hartman, 2018). In mice, *Neurod4* expression promoted the differentiation of excitatory and inhibitory neurons, synapse formation and suppression of GFAP+ astrocytes (Fukuoka et al., 2021). NRG1 is involved in diverse functions such as proliferation, differentiation, and apoptosis of glial and neuronal cells (Liu et al., 2005; Lu et al., 2021). The *NTRK2* gene encodes a member of the neurotrophic tyrosine receptor kinase (NTRK) family and signaling through this kinase (which is a receptor for BDNF and neurotrophin-4) leads to cell differentiation (Bartkowska et al., 2007). *PLP1* encodes a transmembrane proteolipid protein vital for oligodendrocyte development and axonal survival and is used to show presence of oligodendrocyte precursor cells (Venkatesh et al., 2015). *S100B* is a marker of glia cells including astrocytes (e.g. (Koch et al., 2022), and *SOX9* is a transcription factor that plays a role in transmitting pathway signals that regulate astrogliogenesis and astrocyte differentiation (Kang et al., 2011; Martini et al., 2013; Stolt et al., 2003). In the present study, the number of synapses measured by HCI showed a trend towards increase over time (although not statistically significant), whilst our previous studies on the same model reported a more remarkable increase of synapses during differentiation (Davidsen et al., 2021; Pistollato et al., 2020). Despite this discrepancy, the other characterization analyses show that this mixed culture of neurons and astrocytes is generally well suited for testing of DNT in vitro, indicating good transferability and reproducibility of a human hiPSC-derived cell culture model between different laboratories (i.e., from the EC-JRC to NIPH).

To our knowledge, no previous studies have reported effects linked to DNT of GA in cells undergoing differentiation. AA is metabolized to GA by the cytochrome P450 enzyme CYP2E1 (Kraus et al., 2013; Settels et al., 2008), where *CYP2E1* mRNA in the brain show the highest

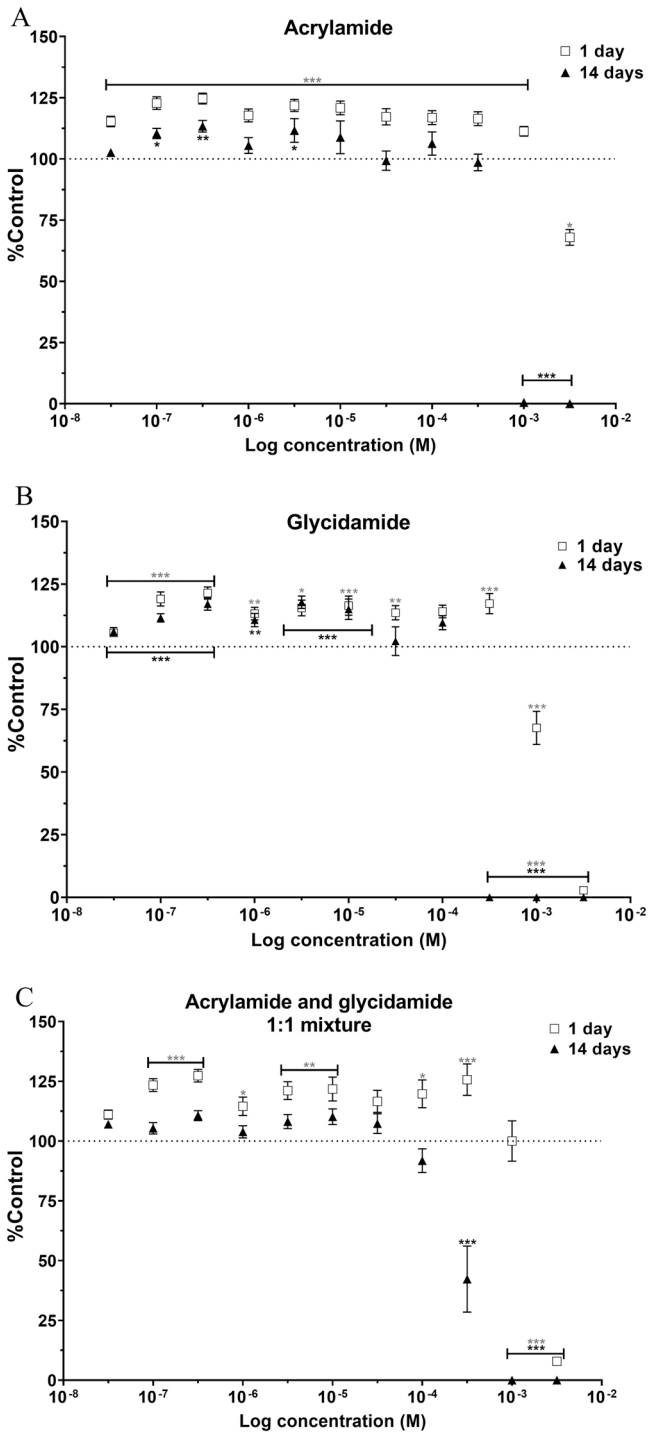

Fig. 5. Toxicity of AA, GA and the combination. Neural stem cells were exposed to a concentration range of AA (A), its metabolite GA (B) and a 1:1 mixture of AA and GA (C) during differentiation. Viability was assessed by mitochondrial activity after 1 and 14 days. The results were normalized to vehicle control cells and data are presented as mean ± S.E.M. of 3–5 independent experiments (cell passages) (* = $p < 0.05$, ** = $p < 0.01$ and *** = $p < 0.001$, compared to control, where black asterisks denote 1 day, and gray asterisks 14 days).

expression levels in cerebellum and cerebral cortex in humans (protein atlas.org). The RNAseq data confirms that *Cyp2E1* is present in our cell culture. Possibly, the toxicity of AA in different species and cell models could reflect the ability to metabolize AA to GA (for review, see e.g. (EFSA, 2015).

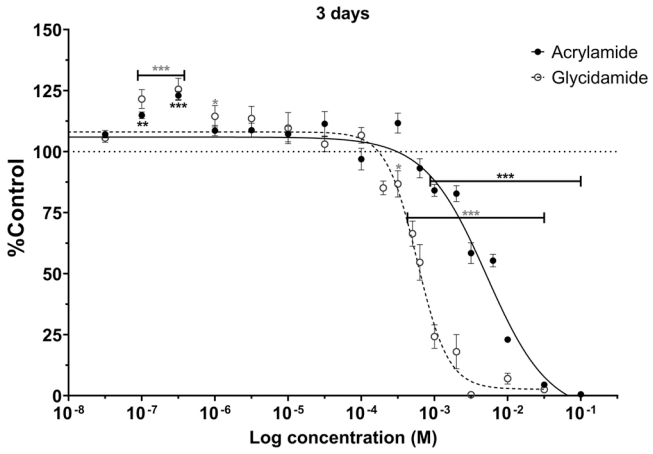

Fig. 6. Concentration - response relationship between exposure to AA and GA for 3 days of differentiation and mitochondrial activity normalized to vehicle control cells. IC_{50} (AA) = 5.2×10^{-3} M and IC_{50} (GA) = 5.8×10^{-4} M was determined by 4-parameter logistical regression. The results were normalized to and compared to vehicle control cells and the data are presented as mean ± S.E.M. of 3–5 independent experiments (cell passages) (* = $p < 0.05$, ** = $p < 0.01$ and *** = $p < 0.001$ compared to the control, where black asterisks denote AA, and gray GA).

Occupational and experimental studies have shown that AA exposure may lead to central and peripheral neurotoxicity, and experimental animal and in vitro studies indicate that developmental exposure to AA may lead to DNT effects. However, the neurodevelopmental processes and mechanisms involved and their possible associations with neurodevelopmental disorders are still not fully understood, particularly since no human studies showing cognitive DNT effects of AA have been performed up to date. "Fundamental neurodevelopmental processes" can be defined as precursor cell proliferation, neuronal and glial cell differentiation and apoptosis, synaptogenesis, myelination, and neurite growth (Bal-Price et al., 2018a; Hoelting et al., 2015; van Thriel et al., 2012), which are necessary for neural network formation and function. DNT compounds may exert their toxicity because they disturb at least one of these processes, which can be modeled in vitro (Aschner et al., 2017; Bal-Price et al., 2015a, 2015b; Davidsen et al., 2021; Kadereit et al., 2012; Lein et al., 2005; van Thriel et al., 2012).

Our study shows that GA was about ten times as potent as AA to induce cell death (IC_{50} values 5.8×10^{-4} M and 5.2×10^{-3} M). Several lines of evidence from in vitro studies support our findings that AA cause neural injury or death (Attoff et al., 2016; Kobolak et al., 2020; Park et al., 2010), as well as altered neurogenesis or gliogenesis (Attoff et al., 2016; Chen and Chou, 2015; Schmuck et al., 2017). AA developmental exposure induced cell death, reduced brain weight or volume in animals (Dortaj et al., 2018; El-Sayyad et al., 2011). Cell injury/death may result in decrease of neuronal network function implied in the impairment of learning and memory (AOP IDs 13, 17, 48, 54) (see e.g. (Spinu et al., 2019).

4.1. *Human relevance of the experimental exposure levels*

Humans are exposed to AA on a daily basis through food, and the plasma concentration levels of unbound AA and GA have been estimated to be around 2 nM and 0.2 nM respectively (peak plasma concentrations) (Young et al., 2007) in humans exposed to 0.23 μg/kg/day. The estimations were based on model considerations since direct measurements from human studies were not available. With an AA intake of 0.6–1.1 μg/kg bw/day (Duarte-Salles et al., 2013; Pedersen et al., 2012) one can roughly assume unbound maximum plasma levels to be around 10 nM. Using Hb adduct levels for calculation of internal dose in terms of area under the curve (AUC), the concentration of free AA over time

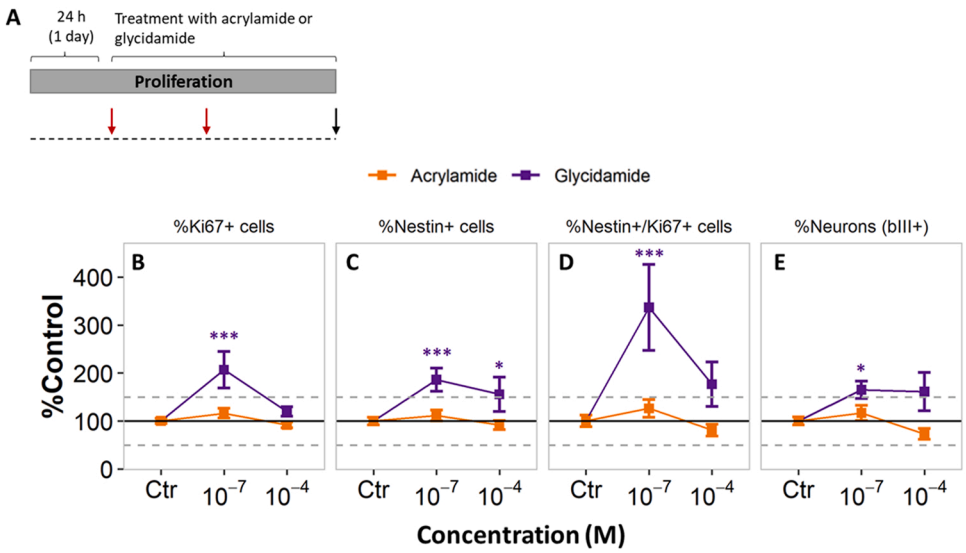

Fig. 7. Detection of proliferation and stem cell markers in neural stem cell cultures undergoing proliferation. (A) Red arrows indicate treatment with AA and GA and black arrow indicates cell fixation and immunocytochemistry. (B) Quantification of Ki67 + proliferating cells, (C) Nestin+ cells, (D) cells co-expressing Nestin+ / Ki67 + and (E) ßIII-Tubulin+ neurons in the cell cultures exposed to 10^{-7} and 10^{-4} M AA and GA in proliferation medium for 7 days. The values are normalized to vehicle control and are presented as mean ± S.E.M. of 3–4 independent experiments (cell passages) (* $p < 0.05$, *** $p < 0.001$ compared to control).

was estimated to 212 nM × h per µg intake of AA/kg bw, where the corresponding AUC for GA was 49 nM × h per µg intake of AA/kg bw (Pedersen et al., 2022; Vikstrom et al., 2011). The estimated AUC's of both AA and GA were higher in humans than for rats (Vikstrom et al., 2011). Assuming similar amounts of AA on both sides of the placenta (Annola et al., 2008; Pedersen et al., 2012; von Stedingk et al., 2011), this may further indicate that DNT effects in vitro at nominal concentrations in the sub micromolar range is relevant for human exposure.

4.2. Acrylamide and glycidamide increased cell proliferation

After 1, 3 and 14 days of differentiation, increased mitochondrial activity (as a measure for viability) was evident in cells exposed to very low concentrations (from 10^{-7} and 3×10^{-7} M) of both AA and GA when compared to control. Increased overall mitochondrial activity in the exposed culture may be due to increased mitochondrial activity occurring because of cellular stress. As proliferation is expected to decrease with differentiation (Davidsen et al., 2021), the enhanced mitochondrial activity seen may also be caused by an inhibition of the differentiation process resulting in a higher number of proliferating cells. Alternatively, an increased cell number may be caused by a reduction of cell death, as apoptosis is an ongoing part of the differentiation process. In Experiment 1 (exposure over 7 days in proliferation cell medium), GA elicited a remarkable increase of proliferating NSCs. Interestingly, AA did not cause such effects. In Experiment 2, after 14 and 28 days of differentiation, increased proliferation (Ki67 + cells) was evident in cells exposed to low concentration (10^{-7} M) of GA (and an increasing trend at 21 days of differentiation). A time-dependent increase in nestin+ cells was observed for GA, and at 14 days only for AA. This shows that GA stimulates proliferation and inhibits differentiation of the neural cells up to 28 days of exposure. The observed increase of proliferation over control levels to a certain extent reproduces autism-like features observed in the brain of ASD children (Courchesne et al., 2011). We have not found any in vitro neurodevelopmental studies on GA exposure and disturbed proliferation and differentiation; however, sustained proliferation in differentiating SH-SY5Y cells have been reported at AA concentrations starting as low as at 10 pM and 10 fM, respectively (Attoff et al., 2016). Attoff and collaborators further reported a reduced number of neurons after AA exposure in the murine neural progenitor cell line C17.2 (Attoff et al., 2016).

4.3. Glycidamide affects brain derived neurotrophic factor, synaptogenesis and gliogenesis

One of the key neurotrophic factors for normal brain development is BDNF, which promotes neuronal survival and plasticity, differentiation, synapse formation and final maturation (Numakawa et al., 2010; Patterson et al., 1996; Poo, 2001; Stansfield et al., 2012). Therefore, any alteration of BDNF levels may impair neuronal differentiation and synaptogenesis, as it has been described in AOP 13: *Chronic binding of antagonist to N-methyl-D-aspartate receptors (NMDARs) during brain development induces impairment of learning and memory abilities* (https://aopwiki.org/wiki/index.php/Aop:13). In these AOPs, reduced BDNF is caused by upstream inhibition of the NMDA receptor, and reduced intracellular calcium (Crozier et al., 2008) (AOP 13), leading to decreased synaptogenesis and neuronal network function, and finally causing impairment in learning and memory (Sachana et al., 2018). The key event relationships identified in these AOPs suggest that chemicals that dysregulate BDNF protein levels, may potentially contribute to impairment of learning and memory in children through mechanisms described in this AOP. In our in vitro study, long-term treatment for 21 and 28 days with GA (but not AA) increased BDNF level, which seemed to increase with differentiation time (day 21–28). These effects were associated with a decrease of synapse number (synaptogenesis), supporting key event relationship 448 (i.e., BDNF dysregulation leads to synaptogenesis dysregulation), as described in AOP-Wiki. It is conceivable that any alterations, i.e., increase or decrease of synaptogenesis and BDNF levels, may in the long term (28 days) lead to compromised neuronal differentiation, possibly resulting in impaired neuronal network formation and function. Interestingly, astrocytes have been shown to express the BDNF receptor tropomyosin receptor kinase B (TrkB), in addition to expressing and releasing BDNF (Fulmer et al., 2014; Holt et al., 2019; Saha et al., 2006), suggesting that astrocytes may contribute to regulation of BDNF availability to neurons (de Pins et al., 2019). The observed increase of BDNF levels could stimulate astrocyte proliferation. In line with this, we observed an up to 3-fold increase of astrocytes after exposure to GA (at 14 and 21 days of differentiation), possibly indicative of activation of neuronal survival mechanisms prompted by astrocytes in our mixed culture of neurons and astrocytes. To our knowledge there are no DNT studies on effects of GA on astrocytes; however, there are some studies showing effects of AA on number of astrocytes. Attoff and collaborators found decreased number of astrocytes or effects on their differentiation in vitro starting at low fM up to low µM concentrations of AA (Attoff et al., 2017, 2020, 2016). Some studies also report effects of AA on glia proliferation in rat offspring

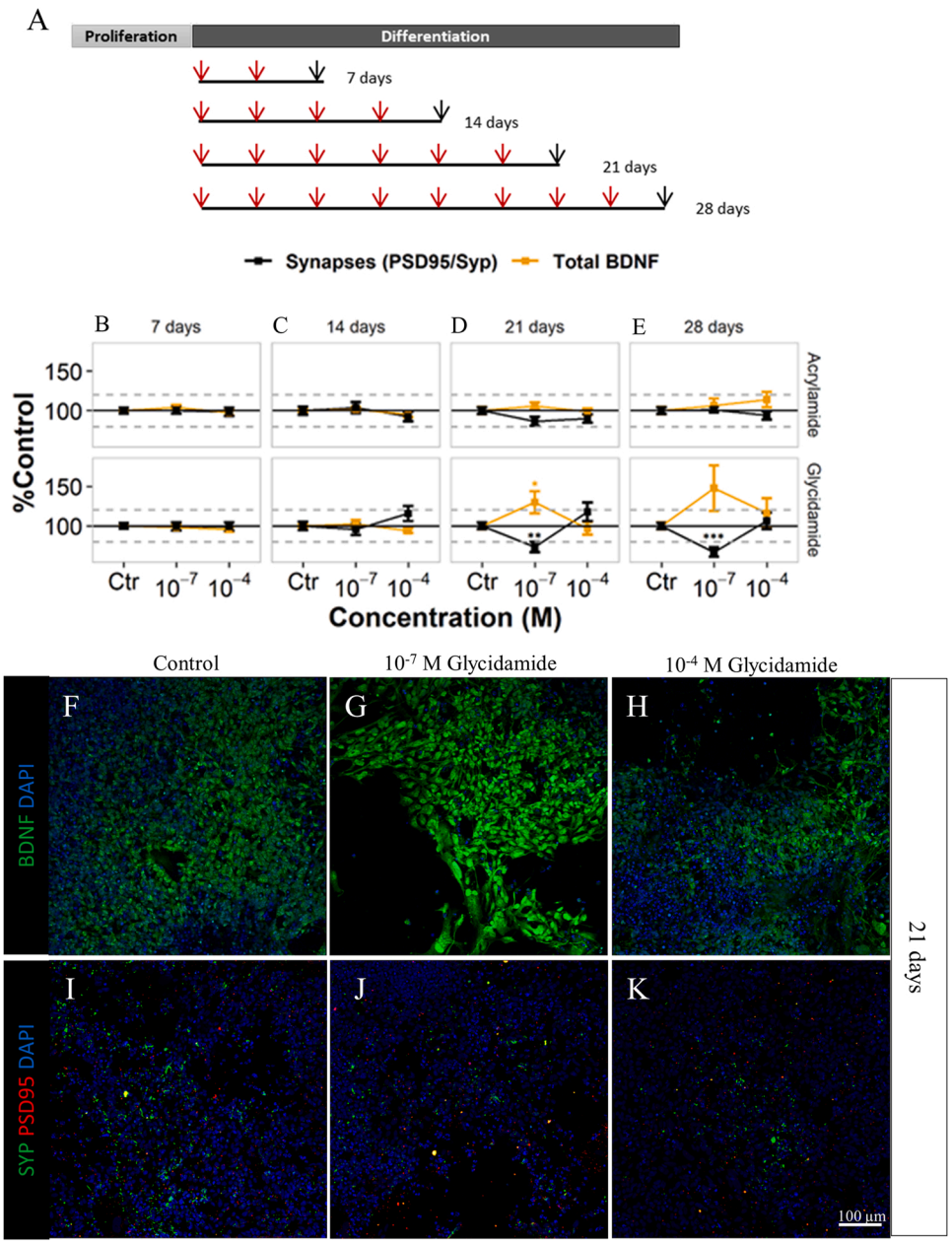

Fig. 8. GA affects BDNF and synapse markers. (A) Red arrows indicate treatment with AA and GA and black arrow indicates cell fixation and immunocytochemistry. (B-E) The curves show quantification of synapses as puncta overlap of PSD95 and SYP, and total BDNF in cells exposed to AA or GA for 7-, 14-, 21- and 28-days. (F - K) Representative immunocytochemical images of control cultures (F and I), and cells treated for 21 days with glycidamide at low concentration (10^{-7} M, G and J) and high concentration (10^{-4} M, H and K). Cells were stained for BDNF (green), in addition to SYP (green, (I - K)) and PSD95 (red, I - K) (10x magnification images). The cell nuclei marker DAPI is shown in blue. The values are normalized to vehicle control and are presented as mean ± S.E.M. of 3–4 independent experiments (cell passages) (** $p < 0.01$, *** $p < 0.001$ compared to the control).

brains after maternal AA exposure (Allam et al., 2011; Ogawa et al., 2012). Alterations of astrocyte proportion may affect neurobehavior in animals; Nagai et al. found that activation of Gi-mediated GPCR signaling in striatal astrocytes altered mouse behavior (Nagai et al., 2019). Astrocytes are also crucial for processes like memory formation and mood-associated behaviors (including anxiety disorders) reviewed in (Park and Lee, 2020).

Decrease of synaptogenesis has been reported after intragastric AA exposure (GD 6–21) in rats (Lai et al., 2017), while both in vitro and in vivo studies have shown reduced BDNF (Attoff et al., 2020; Erdemli et al., 2018, 2016) (contrary to our in vitro observations), which could affect synaptogenesis (Aschner et al., 2017). Others have found altered gene expression for reduced synaptogenesis, neural network formation and differentiation in C17.2 NP cells (Attoff et al., 2017) and in SH -SY5Y cells (Attoff et al., 2020).

4.4. GA disturbed neurite growth and neural maturation

To reveal possible effects on differentiation and maturation of our mixed neuronal and astrocyte culture, ßIII-Tubulin was used as a marker for immature neurons and neurites and Map2 as a marker for more committed and fully developed neurons and neurites. Since Map2 + neurite branch points and neurites per neuron decreased during differentiation, while βII-Tubulin+ percent of neurons, branch points, neurite length and neurites per neuron increased, the data indicate disturbed maturation of neurons and thereby decreased differentiation. This may partly be explained by the increased BDNF expression after exposure to GA, since BDNF signaling is involved in synapse and neural maturation (Ehrlich and Josselyn, 2016). To our knowledge no studies have previously reported GA-induced effects on neurite outgrowth or arborization; however, multiple studies have revealed impaired neurite growth and maturation after AA exposure (Attoff et al., 2017, 2020, 2016; Lee et al., 2018). These disturbed processes induced by GA may have some relevance for neurodevelopmental disorders, since mutations

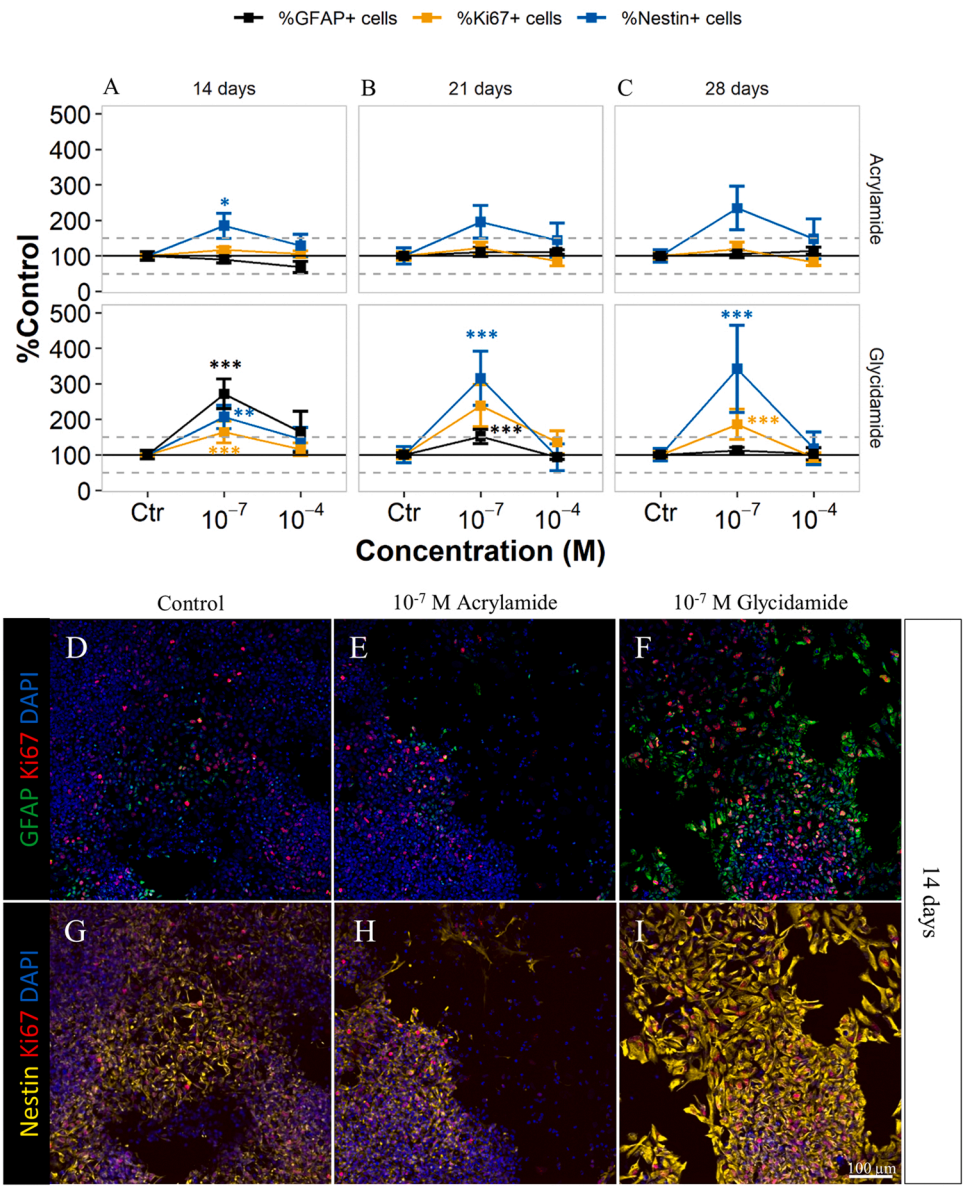

Fig. 9. Effects of AA and GA on proliferation, neural differentiation and astrocyte markers. (A – C) Quantification of astrocytes indicated by %GFAP+ cells, cells in proliferation and NSCs indicated by %nestin+ cells after treatment with AA and GA for 14-, 21- and 28-days during differentiation. (D - I) Representative immunocytochemical images of control culture (D and G), and cells treated for 14 days with acrylamide (10^{-7} M, E and H) and glycidamide (10^{-7} M, F and I). NSCs were stained with GFAP (green) and Ki67 (red) (D - F), in addition to nestin (yellow) combined with Ki67 (red) (G - I). The cell nuclei marker DAPI is shown in blue (10x magnification images). Results are normalized to vehicle control and are presented as mean ± S.E.M. of 3–4 independent experiments (cell passages) (* $p < 0.05$, ** $p < 0.01$, *** $p < 0.001$ compared to control).

in certain genes of autism spectrum disorder patients converge on cellular pathways that intercept at synapses (Guang et al., 2018), and abnormal neurite formation between adjacent cells which may cause impairment of the ability to integrate the information arriving from different brain regions (Courchesne and Pierce, 2005).

4.5. *Impaired neurodevelopmental processes and behavioral deficits*

Impaired synaptogenesis can negatively affect neural network formation and function, resulting in memory impairment which is an adverse outcome in the AOP framework for neurodevelopmental toxicity (Spinu et al., 2019). Some studies in rats have actually reported behavioral effects in the offspring developmentally exposed to AA, like deceased cognitive motivation (food reinforcement tests) (Garey and Paule, 2007, 2010), anxiogenic responses in the elevated plus maze and in the open field test (Ferguson et al., 2010; Krishna and Muralidhara, 2018), impaired motor activity or coordination shown as negative geotaxis performance and deceased fall time latency in the rotarod test (Garey et al., 2005), in addition to decreases in average horizontal motor activity and auditory startle response (Wise et al., 1995). According to (Aschner et al., 2017), cell biological causes of such effects could be e.g., decreased synaptogenesis and network formation, in addition to specific death of neuronal subpopulations, providing biological plausibility to these behavioral effects observed in rat offspring. Our findings are therefore examples of events relevant for AOPs linking exposure to DNT chemicals to human toxicity. However, more information from human studies on functional cognitive endpoints are needed to confirm these experimental findings since the observed effects of AA on head circumference and birth weight (Duarte-Salles et al., 2013; Pedersen et al., 2012) may also be indirect consequences of toxicity.

Fig. 11 summarizes the fundamental neurodevelopmental processes (vital for normal brain development) which are disturbed in the human NSC model after exposure to low concentrations of AA and/or GA.

5. Conclusion

Our results show that AA and GA at low concentration (1×10^{-7}) increased cell viability both in immature and differentiating human NSCs. Increased BDNF with decreased synaptogenesis and increased number of astrocytes in the mixed culture of neurons and astrocytes were observed upon exposure to GA only at later differentiation stages. AA showed tendency towards decreased differentiation (increased

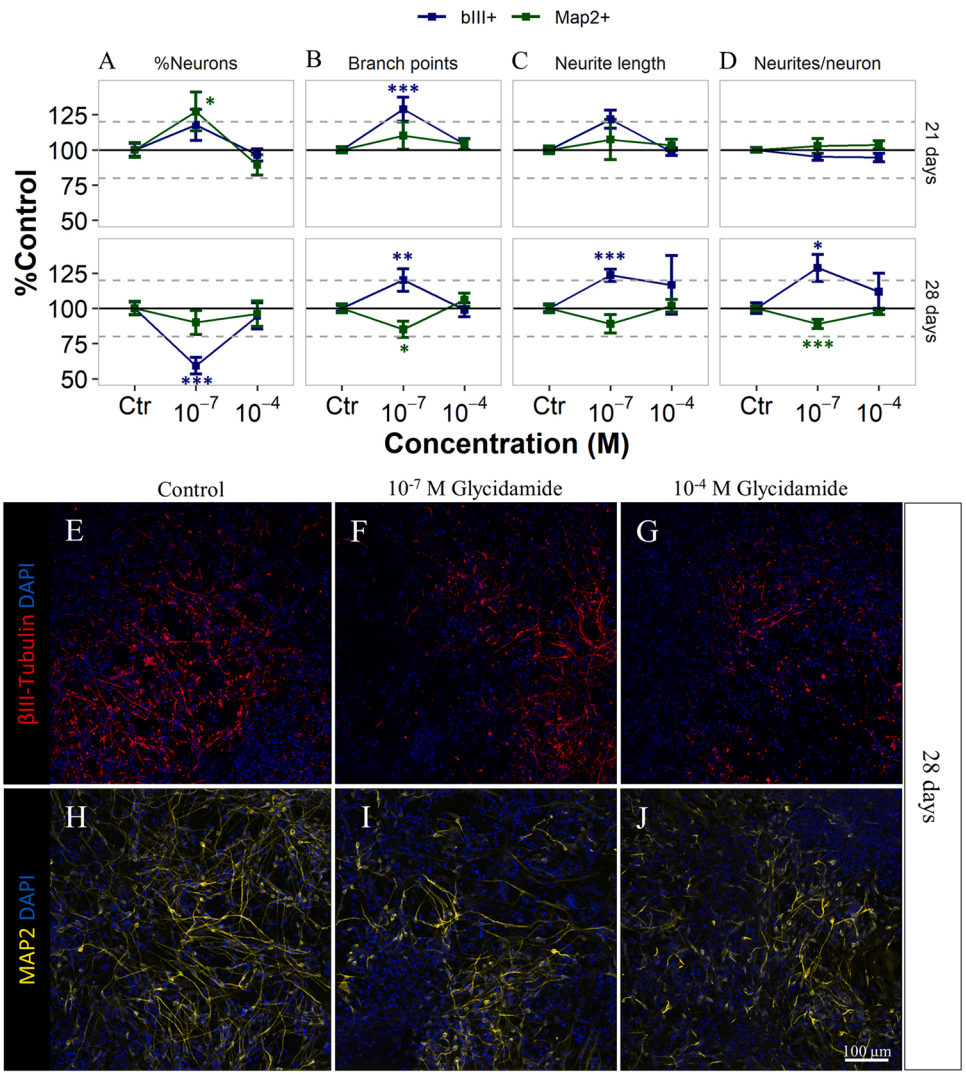

Fig. 10. Markers of neurite growth and neural maturation. (A-D) The upper figure shows quantification of %neurons, arborization, neurite length, and number of neurites per neuron in NSCs exposed to 10^{-7} and 10^{-4} M GA during differentiation for 21 and 28 days. Blue lines indicate neurite outgrowth quantified by ßIII-Tubulin staining and green lines indicate the same quantification by Map2 staining. (E-J) Representative immunocytochemical images of control cultures (E and H), and cells treated for 21 and 28 days with glycidamide at low concentration (10^{-7} M, F and I) and high concentration (10^{-4} M, G and J). Cells were stained for β-III-Tubulin (red), and Map2 (yellow). The cell nuclei marker DAPI is shown in blue (10x magnification images). The values are normalized to vehicle control and are presented as mean ± S.E.M. of 3–4 independent experiments (cell passages) (* $p < 0.05$, ** $p < 0.01$, *** $p < 0.001$ compared to control).

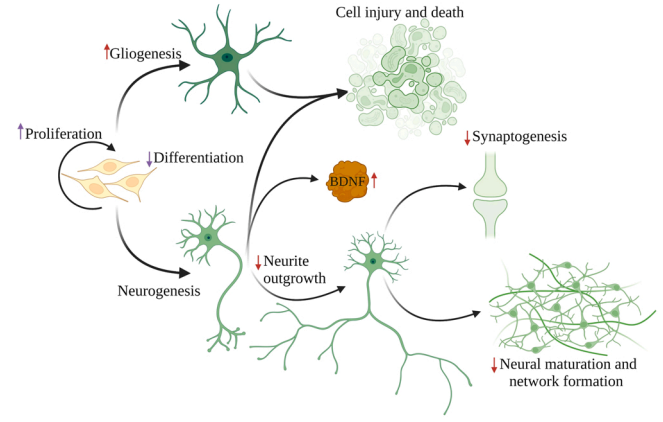

Fig. 11. Overview of the fundamental neurodevelopmental processes affected by exposure to AA (increased proliferation and decreased differentiation) and/or its main metabolite glycidamide (increased proliferation and gliogenesis, in addition to impaired differentiation, neurite outgrowth, synaptogenesis, network formation) in a human mixed culture of neurons and astrocytes undergoing differentiation up to 28 days (red arrows; glycidamide effects, purple arrows; effects induced by both compounds). Disturbance of any of these processes in the developing brain may lead to impairment of learning, memory, and cognitive processes in the child. Figure created with BioRender.com.

nestin+). Since Map2 + neurite branch points and neurites per neuron decreased during differentiation, while βIII-Tubulin+ percent of neurons, branch points, neurite length and neurites per neuron increased, the data further show disturbed commitment to mature neurons and decreased neuronal differentiation. The effects in vitro seen in the sub or low micromolar range is relevant for human exposure. Disturbance of any of these processes in the developing brain may lead to impairment of cognitive processes in the child.

Funding

This research did not receive any specific grant from funding agencies in the public, commercial, or not-for-profit sectors.

CRediT authorship contribution statement

Anna Jacobsen Lauvås: Conceptualization, Formal analysis, Investigation, Writing – original draft, Writing – review & editing, Visualization. **Malene Lislien:** Conceptualization, Methodology, Formal analysis, Investigation, Writing – original draft, Writing – review & editing, Visualization. **Hubert Dirven:** Conceptualization, Writing – review & editing, Resources, Funding acquisition. **Jørn Andreas Holme:** Conceptualization, Investigation, Methodology, Writing – review & editing. **Ragnhild Elisabeth Paulsen:** Conceptualization, Writing – review & editing. **Inger Margit Alm:** Conceptualization,

Methodology, Investigation, Writing – review & editing. **Ellen Skarpen:** Conceptualization, Formal analysis, Methodology, Writing – review & editing. **Jill Mari Andersen:** Investigation, Methodology, Writing – review & editing. **Vigdis Sørensen:** Conceptualization, Formal analysis, Methodology, Investigation, Writing – review & editing. **Peter Macko:** Formal analysis, Methodology, Writing – review & editing. **Francesca Pistollato:** Supervision, Formal analysis, Methodology, Investigation, Writing – review & editing. **Nur Duale:** Formal analysis, Methodology, Writing – original draft, Writing – review & editing. **Oddvar Myhre:** Conceptualization, Supervision, Methodology, Investigation, Writing – review & editing.

Declaration of Competing Interest

The authors declare that they have no known competing financial interests or personal relationships that could have appeared to influence the work reported in this paper.

Acknowledgments

The authors would like to thank Tone Rasmussen and Tonje Skuland for their contributions in the lab, Anna Bal-Price and Maurice Whelan (EC-JRC, Ispra) for the collaboration and transfer of the cell model from EC-JRC to NIPH.

Appendix A. Supplementary material

Supplementary data associated with this article can be found in the online version at doi:10.1016/j.neuro.2022.07.001.

References

Aarem, J., Brunborg, G., Aas, K.K., Harbak, K., Taipale, M.M., Magnus, P., Knudsen, G.P., Duale, N., 2016. Comparison of blood RNA isolation methods from samples stabilized in Tempus tubes and stored at a large human biobank. BMC Res. Notes 9 (1), 430.

Allam, A., El-Ghareeb, A.A., Abdul-Hamid, M., Baikry, A., Sabri, M.I., 2011. Prenatal and perinatal acrylamide disrupts the development of cerebellum in rat: biochemical and morphological studies. Toxicol. Ind. Health 27, 291–306.

Allam, A., El-Gareeb, A., Ajarem, J., Abdul-Hamid, M., El-Bakry, A., 2013. Effect of acrylamide on the development of medulla oblongata in albino rat: biochemical and morphological studies. Afr. J. Pharm. Pharmacol. 7, 1320–1331.

Andersen, H.R., Nielsen, J.B., Grandjean, P., 2000. Toxicologic evidence of developmental neurotoxicity of environmental chemicals. Toxicology 144 (1–3), 121–127.

Annola, K., Karttunen, V., Keski-Rahkonen, P., Myllynen, P., Segerbäck, D., Heinonen, S., Vähäkangas, K., 2008. Transplacental transfer of acrylamide and glycidamide are comparable to that of antipyrine in perfused human placenta. Toxicol. Lett. 182 (1–3), 50–56.

Aschner, M., Ceccatelli, S., Daneshian, M., Fritsche, E., Hasiwa, N., Hartung, T., Hogberg, H.T., Leist, M., Li, A., Mundi, W.R., Padilla, S., Piersma, A.H., Bal-Price, A., Seiler, A., Westerink, R.H., Zimmer, B., Lein, P.J., 2017. Reference compounds for alternative test methods to indicate developmental neurotoxicity (DNT) potential of chemicals: example lists and criteria for their selection and use. Altex 34 (1), 49–74.

Attoff, K., Kertika, D., Lundqvist, J., Oredsson, S., Forsby, A., 2016. Acrylamide affects proliferation and differentiation of the neural progenitor cell line C17.2 and the neuroblastoma cell line SH-SY5Y. Toxicol. Vitr. 35, 100–111.

Attoff, K., Gliga, A., Lundqvist, J., Norinder, U., Forsby, A., 2017. Whole genome microarray analysis of neural progenitor C17.2 cells during differentiation and validation of 30 neural mRNA biomarkers for estimation of developmental neurotoxicity. PLoS One 12 (12), e0190066.

Attoff, K., Johansson, Y., Cediel-Ulloa, A., Lundqvist, J., Gupta, R., Caiment, F., Gliga, A., Forsby, A., 2020. Acrylamide alters CREB and retinoic acid signalling pathways during differentiation of the human neuroblastoma SH-SY5Y cell line. Sci. Rep. 10 (1), 16714.

Bal-Price, A., Crofton, K.M., Leist, M., Allen, S., Arand, M., Buetler, T., Delrue, N., FitzGerald, R.E., Hartung, T., Heinonen, T., Hogberg, H., Bennekou, S.H., Lichtensteiger, W., Oggier, D., Paparella, M., Axelstad, M., Piersma, A., Rached, E., Schilter, B., Schmuck, G., Stoppini, L., Tongiorgi, E., Tiramani, M., Monnet-Tschudi, F., Wilks, M.F., Ylikomi, T., Fritsche, E., 2015a. International STakeholder NETwork (ISTNET): creating a developmental neurotoxicity (DNT) testing road map for regulatory purposes. Arch. Toxicol. 89 (2), 269–287.

Bal-Price, A., Crofton, K.M., Sachana, M., Shafer, T.J., Behl, M., Forsby, A., Hargreaves, A., Landesmann, B., Lein, P.J., Louisse, J., Monnet-Tschudi, F., Paini, A., Rolaki, A., Schrattenholz, A., Suñol, C., van Thriel, C., Whelan, M., Fritsche, E., 2015b. Putative adverse outcome pathways relevant to neurotoxicity. Crit. Rev. Toxicol. 45 (1), 83–91.

Bal-Price, A., Hogberg, H.T., Crofton, K.M., Daneshian, M., FitzGerald, R.E., Fritsche, E., Heinonen, T., Hougaard Bennekou, S., Klima, S., Piersma, A.H., Sachana, M., Shafer, T.J., Terron, A., Monnet-Tschudi, F., Viviani, B., Waldmann, T., Westerink, R. H.S., Wilks, M.F., Witters, H., Zurich, M.G., Leist, M., 2018a. Recommendation on test readiness criteria for new approach methods in toxicology: exemplified for developmental neurotoxicity. Altex 35 (3), 306–352.

Bal-Price, A., Pistollato, F., Sachana, M., Bopp, S.K., Munn, S., Worth, A., 2018b. Strategies to improve the regulatory assessment of developmental neurotoxicity (DNT) using in vitro methods. Toxicol. Appl. Pharmacol. 354, 7–18.

Bartkowska, K., Paquin, A., Gauthier, A.S., Kaplan, D.R., Miller, F.D., 2007. Trk signaling regulates neural precursor cell proliferation and differentiation during cortical development. Development 134 (24), 4369–4380.

Bušová, M., Bencko, V., Veszelits Laktičová, K., Holcátová, I., Vargová, M., 2020. Risk of exposure to acrylamide. Cent. Eur. J. Public Health Suppl. 28, S43–S46.

Chen, J.H., Chou, C.C., 2015. Acrylamide inhibits cellular differentiation of human neuroblastoma and glioblastoma cells. Food Chem. Toxicol. 82, 27–35.

Chen, J.H., Lee, D.C., Chiu, I.M., 2014. Cytotoxic effects of acrylamide in nerve growth factor or fibroblast growth factor 1-induced neurite outgrowth in PC12 cells. Arch. Toxicol. 88 (3), 769–780.

Chung, D., Shum, A., Caraveo, G., 2020. GAP-43 and BASP1 in axon regeneration: implications for the treatment of neurodegenerative diseases. Front. Cell Dev. Biol. 8, 567537.

Courchesne, E., Pierce, K., 2005. Why the frontal cortex in autism might be talking only to itself: local over-connectivity but long-distance disconnection. Curr. Opin. Neurobiol. 15 (2), 225–230.

Courchesne, E., Mouton, P.R., Calhoun, M.E., Semendeferi, K., Ahrens-Barbeau, C., Hallet, M.J., Barnes, C.C., Pierce, K., 2011. Neuron number and size in prefrontal cortex of children with autism. JAMA 306 (18), 2001–2010.

Crofton, K.M., Mundy, W.R., 2021. External Scientific Report on the Interpretation of Data from the Developmental Neurotoxicity In Vitro Testing Assays for Use in Integrated Approaches for Testing and Assessment. EFSA Supporting Publications, p. 18. https://doi.org/10.2903/sp.efsa.2021.EN-6924.

Crozier, R.A., Bi, C., Han, Y.R., Plummer, M.R., 2008. BDNF modulation of NMDA receptors is activity dependent. J. Neurophysiol. 100 (6), 3264–3274.

Davidsen, N., Lauvås, A.J., Myhre, O., Ropstad, E., Carpi, D., Gyves, E.M., Berntsen, H.F., Dirven, H., Paulsen, R.E., Bal-Price, A., Pistollato, F., 2021. Exposure to human relevant mixtures of halogenated persistent organic pollutants (POPs) alters neurodevelopmental processes in human neural stem cells undergoing differentiation. Reprod. Toxicol. 100, 17–34.

Dearfield, K.L., Abernathy, C.O., Ottley, M.S., Brantner, J.H., Hayes, P.F., 1988. Acrylamide: its metabolism, developmental and reproductive effects, genotoxicity, and carcinogenicity. Mutat. Res. 195 (1), 45–77.

Di Consiglio, E., Pistollato, F., Mendoza-De Gyves, E., Bal-Price, A., Testai, E., 2020. Integrating biokinetics and in vitro studies to evaluate developmental neurotoxicity induced by chlorpyrifos in human iPSC-derived neural stem cells undergoing differentiation towards neuronal and glial cells. Reprod. Toxicol. 98, 174–188.

Dortaj, H., Yadegari, M., Hosseini Sharif Abad, M., Abbasi Sarcheshmeh, A., Anvari, M., 2018. Stereological method for assessing the effect of vitamin C administration on the reduction of acrylamide-induced neurotoxicity. Basic Clin. Neurosci. 9 (1), 27–34.

Duale, N., Olsen, A.K., Christensen, T., Butt, S.T., Brunborg, G., 2010. Octyl methoxycinnamate modulates gene expression and prevents cyclobutane pyrimidine dimer formation but not oxidative DNA damage in UV-exposed human cell lines. Toxicol. Sci. 114 (2), 272–284.

Duale, N., Brunborg, G., Rønningen, K.S., Briese, T., Aarem, J., Aas, K.K., Magnus, P., Stoltenberg, C., Susser, E., Lipkin, W.I., 2012. Human blood RNA stabilization in samples collected and transported for a large biobank. BMC Res. Notes 5, 510.

Duale, N., Lipkin, W.I., Briese, T., Aarem, J., Rønningen, K.S., Aas, K.K., Magnus, P., Harbak, K., Susser, E., Brunborg, G., 2014. Long-term storage of blood RNA collected in RNA stabilizing Tempus tubes in a large biobank–evaluation of RNA quality and stability. BMC Res. Notes 7, 633.

Duarte-Salles, T., von Stedingk, H., Granum, B., Gützkow, K.B., Rydberg, P., Törnqvist, M., Mendez, M.A., Brunborg, G., Brantsæter, A.L., Meltzer, H.M., Alexander, J., Haugen, M., 2013. Dietary acrylamide intake during pregnancy and fetal growth-results from the Norwegian mother and child cohort study (MoBa). Environ. Health Perspect. 121 (3), 374–379.

EFSA, 2015. CONTAM panel (EFSA panel on contaminants in the food chain). Scientific opinion on acrylamide in food. EFSA J. 13 (6), 4104. https://doi.org/10.2903/j.efsa.2015.4104. EFSA Journal 2015;13(6):4104.

Ehrlich, D.E., Josselyn, S.A., 2016. Plasticity-related genes in brain development and amygdala-dependent learning. Genes Brain Behav. 15 (1), 125–143.

El-Sayyad, H.I., El-Gammal, H.L., Habak, L.A., Abdel-Galil, H.M., Fernando, A., Gaur, R. L., Ouhtit, A., 2011. Structural and ultrastructural evidence of neurotoxic effects of fried potato chips on rat postnatal development. Nutrition 27 (10), 1066–1075.

Erdemli, M.E., Turkoz, Y., Altinoz, E., Elibol, E., Dogan, Z., 2016. Investigation of the effects of acrylamide applied during pregnancy on fetal brain development in rats and protective role of the vitamin E. Hum. Exp. Toxicol. 35 (12), 1337–1344.

Erdemli, M.E., Arif Aladag, M., Altinoz, E., Demirtas, S., Turkoz, Y., Yigitcan, B., Bag, H. G., 2018. Acrylamide applied during pregnancy causes the neurotoxic effect by lowering BDNF levels in the fetal brain. Neurotoxicol. Teratol. 67, 37–43.

Erkekoglu, P., Baydar, T., 2014. Acrylamide neurotoxicity. Nutr. Neurosci. 17 (2), 49–57.

Ferguson, S.A., Garey, J., Smith, M.E., Twaddle, N.C., Doerge, D.R., Paule, M.G., 2010. Preweaning behaviors, developmental landmarks, and acrylamide and glycidamide

levels after pre- and postnatal acrylamide treatment in rats. Neurotoxicol. Teratol. 32 (3), 373–382.
Friedman, M., 2003. Chemistry, biochemistry, and safety of acrylamide. A review. J. Agric. Food Chem. 51 (16), 4504–4526.
Fritsche, E., Grandjean, P., Crofton, K.M., Aschner, M., Goldberg, A., Heinonen, T., Hessel, E.V.S., Hogberg, H.T., Bennekou, S.H., Lein, P.J., Leist, M., Mundy, W.R., Paparella, M., Piersma, A.H., Sachana, M., Schmuck, G., Solecki, R., Terron, A., Monnet-Tschudi, F., Wilks, M.F., Witters, H., Zurich, M.G., Bal-Price, A., 2018. Consensus statement on the need for innovation, transition and implementation of developmental neurotoxicity (DNT) testing for regulatory purposes. Toxicol. Appl. Pharmacol. 354, 3–6.
Fritsche, E., Tigges, J., Hartmann, J., Kapr, J., Serafini, M.M., Viviani, B., 2021. Neural in vitro models for studying substances acting on the central nervous system. Handb. Exp. Pharmacol. 265, 111–141.
Fukuoka, T., Kato, A., Hirano, M., Ohka, F., Aoki, K., Awaya, T., Adilijiang, A., Sachi, M., Tanahashi, K., Yamaguchi, J., Motomura, K., Shimizu, H., Nagashima, Y., Ando, R., Wakabayashi, T., Lee-Liu, D., Larrain, J., Nishimura, Y., Natsume, A., 2021. Neurod4 converts endogenous neural stem cells to neurons with synaptic formation after spinal cord injury. iScience 24 (2), 102074.
Fulmer, C.G., VonDran, M.W., Stillman, A.A., Huang, Y., Hempstead, B.L., Dreyfus, C.F., 2014. Astrocyte-derived BDNF supports myelin protein synthesis after cuprizone-induced demyelination. J. Neurosci. 34 (24), 8186–8196.
Garey, J., Paule, M.G., 2007. Effects of chronic low-dose acrylamide exposure on progressive ratio performance in adolescent rats. Neurotoxicology 28 (5), 998–1002.
Garey, J., Paule, M.G., 2010. Effects of chronic oral acrylamide exposure on incremental repeated acquisition (learning) task performance in Fischer 344 rats. Neurotoxicol. Teratol. 32 (2), 220–225.
Garey, J., Ferguson, S.A., Paule, M.G., 2005. Developmental and behavioral effects of acrylamide in Fischer 344 rats. Neurotoxicol. Teratol. 27 (4), 553–563.
Ghanayem, B.I., McDaniel, L.P., Churchwell, M.I., Twaddle, N.C., Snyder, R., Fennell, T. R., Doerge, D.R., 2005. Role of CYP2E1 in the epoxidation of acrylamide to glycidamide and formation of DNA and hemoglobin adducts. Toxicol. Sci. 88 (2), 311–318.
Grandjean, P., Landrigan, P.J., 2006. Developmental neurotoxicity of industrial chemicals. Lancet 368 (9553), 2167–2178.
Granvogl, M., Koehler, P., Latzer, L., Schieberle, P., 2008. Development of a stable isotope dilution assay for the quantitation of glycidamide and its application to foods and model systems. J. Agric. Food Chem. 56 (15), 6087–6092.
Guang, S., Pang, N., Deng, X., Yang, L., He, F., Wu, L., Chen, C., Yin, F., Peng, J., 2018. Synaptopathology involved in autism spectrum disorder. Front. Cell. Neurosci. 12, 470.
Hagmar, L., Törnqvist, M., Nordander, C., Rosén, I., Bruze, M., Kautiainen, A., Magnusson, A.L., Malmberg, B., Aprea, P., Granath, F., Axmon, A., 2001. Health effects of occupational exposure to acrylamide using hemoglobin adducts as biomarkers of internal dose. Scand. J. Work Environ. Health 27 (4), 219–226.
Hessel, E.V.S., Staal, Y.C.M., Piersma, A.H., 2018. Design and validation of an ontology-driven animal-free testing strategy for developmental neurotoxicity testing. Toxicol. Appl. Pharmacol. 354, 136–152.
Hoelting, L., Leist, M., Stoppini, L., 2015. Using pluripotent stem cells and their progeny as an in vitro model to assess (developmental) neurotoxicity. In: Pfannkuch, F., Suter-Dick, L. (Eds.), Predictive Toxicology: From Vision to Reality. Wiley-VCH Verlag GmbH & Co. KGaA, Weinheim, Germany.
Hogberg, H.T., Kinsner-Ovaskainen, A., Hartung, T., Coecke, S., Bal-Price, A.K., 2009. Gene expression as a sensitive endpoint to evaluate cell differentiation and maturation of the developing central nervous system in primary cultures of rat cerebellar granule cells (CGCs) exposed to pesticides. Toxicol. Appl. Pharmacol. 235 (3), 268–286.
Hogberg, H.T., Kinsner-Ovaskainen, A., Coecke, S., Hartung, T., Bal-Price, A.K., 2010. mRNA expression is a relevant tool to identify developmental neurotoxicants using an in vitro approach. Toxicol. Sci. 113 (1), 95–115.
Holt, L.M., Hernandez, R.D., Pacheco, N.L., Torres Ceja, B., Hossain, M., Olsen, M.L., 2019. Astrocyte morphogenesis is dependent on BDNF signaling via astrocytic TrkB. T1. eLife 8.
IARC, 1994. Acrylamide. IARC Monographs on the Evaluation of Carcinogenic Risks to Humans. International Agency for Research on Cancer, pp. 389–433.
JECFA, 2005. JECFA, Joint FAO/WHO Expert Committee on Food Additives. WHO/FAO, Rome, p. 47.
Kadereit, S., Zimmer, B., van Thriel, C., Hengstler, J.G., Leist, M., 2012. Compound selection for in vitro modeling of developmental neurotoxicity. Front Biosci. 17, 2442–2460.
Kang, H.J., Kawasawa, Y.I., Cheng, F., Zhu, Y., Xu, X., Li, M., Sousa, A.M., Pletikos, M., Meyer, K.A., Sedmak, G., Guennel, T., Shin, Y., Johnson, M.B., Krsnik, Z., Mayer, S., Fertuzinhos, S., Umlauf, S., Lisgo, S.N., Vortmeyer, A., Weinberger, D.R., Mane, S., Hyde, T.M., Huttner, A., Reimers, M., Kleinman, J.E., Sestan, N., 2011. Spatio-temporal transcriptome of the human brain. Nature 478 (7370), 483–489.
Kim, D., Paggi, J.M., Park, C., Bennett, C., Salzberg, S.L., 2019. Graph-based genome alignment and genotyping with HISAT2 and HISAT-genotype. Nat. Biotechnol. 37 (8), 907–915.
Kim, T.H., Shin, S., Kim, K.B., Seo, W.S., Shin, J.C., Choi, J.H., Weon, K.Y., Joo, S.H., Jeong, S.W., Shin, B.S., 2015. Determination of acrylamide and glycidamide in various biological matrices by liquid chromatography-tandem mass spectrometry and its application to a pharmacokinetic study. Talanta 131, 46–54.
Kleinjans, J., Botsivali, M., Kogevinas, M., Merlo, D.F., 2015. Fetal exposure to dietary carcinogens and risk of childhood cancer: what the NewGeneris project tells us. BMJ 351, h4501.
Kobolak, J., Teglasi, A., Bellak, T., Janstova, Z., Molnar, K., Zana, M., Bock, I., Laszlo, L., Dinnyes, A., 2020. Human induced pluripotent stem cell-derived 3D-neurospheres are suitable for neurotoxicity screening. Cells 9 (5).
Koch, K., Bartmann, K., Hartmann, J., Kapr, J., Klose, J., Kuchovská, E., Pahl, M., Schlüppmann, K., Zühr, E., Fritsche, E., 2022. Scientific validation of human neurosphere assays for developmental neurotoxicity evaluation. Front. Toxicol. 4.
Kraus, D., Rokitta, D., Fuhr, U., Tomalik-Scharte, D., 2013. The role of human cytochrome P450 enzymes in metabolism of acrylamide in vitro. Toxicol. Mech. Methods 23 (5), 346–351.
Krishna, G., Muralidhara, 2018. Oral supplements of combined fructo- and xylo-oligosaccharides during perinatal period significantly offsets acrylamide-induced oxidative impairments and neurotoxicity in rats. J. Physiol. Pharmacol. 69 (5).
Krishna, G., Divyashri, G., Prapulla, S.G., Muralidhara, 2015. A combination supplement of fructo- and xylo-oligosaccharides significantly abrogates oxidative impairments and neurotoxicity in maternal/fetal milieu following gestational exposure to acrylamide in rat. Neurochem. Res. 40 (9), 1904–1918.
Krug, A.K., Balmer, N.V., Matt, F., Schönenberger, F., Merhof, D., Leist, M., 2013. Evaluation of a human neurite growth assay as specific screen for developmental neurotoxicants. Arch. Toxicol. 87 (12), 2215–2231.
Kütting, B., Schettgen, T., Schwegler, U., Fromme, H., Uter, W., Angerer, J., Drexler, H., 2009. Acrylamide as environmental noxious agent: a health risk assessment for the general population based on the internal acrylamide burden. Int. J. Hyg. Environ. Health 212 (5), 470–480.
Lai, S.M., Gu, Z.T., Zhao, M.M., Li, X.X., Ma, Y.X., Luo, L., Liu, J., 2017. Toxic effect of acrylamide on the development of hippocampal neurons of weaning rats. Neural Regen. Res. 12 (10), 1648–1654.
Lee, S., Park, H.R., Lee, J.Y., Cho, J.H., Song, H.M., Kim, A.H., Lee, W., Lee, Y., Chang, S. C., Kim, H.S., Lee, J., 2018. Learning, memory deficits, and impaired neuronal maturation attributed to acrylamide. J. Toxicol. Environ. Health A 81 (9), 254–265.
Lein, P., Silbergeld, E., Locke, P., Goldberg, A.M., 2005. In vitro and other alternative approaches to developmental neurotoxicity testing (DNT). Environ. Toxicol. Pharmacol. 19 (3), 735–744.
Liao, Y., Smyth, G.K., Shi, W., 2014. featureCounts: an efficient general purpose program for assigning sequence reads to genomic features. Bioinformatics 30 (7), 923–930.
LiCausi, F., Hartman, N.W., 2018. Role of mTOR complexes in neurogenesis. Int. J. Mol. Sci. 19, 5.
Lindeman, B., Johansson, Y., Andreassen, M., Husøy, T., Dirven, H., Hofer, T., Knutsen, H.K., Caspersen, I.H., Vejrup, K., Paulsen, R.E., Alexander, J., Forsby, A., Myhre, O., 2021. Does the food processing contaminant acrylamide cause developmental neurotoxicity? A review and identification of knowledge gaps. Reprod. Toxicol. 101, 93–114.
Liu, Y., Ford, B.D., Mann, M.A., Fischbach, G.D., 2005. Neuregulin-1 increases the proliferation of neuronal progenitors from embryonic neural stem cells. Dev. Biol. 283 (2), 437–445.
Livak, K.J., Schmittgen, T.D., 2001. Analysis of relative gene expression data using real-time quantitative PCR and the 2(-Delta Delta C(T)) Method. Methods 25 (4), 402–408.
Love, M.I., Huber, W., Anders, S., 2014. Moderated estimation of fold change and dispersion for RNA-seq data with DESeq2. Genome Biol. 15 (12), 550.
Lu, F., Wei, L., Yang, C., Qiao, Y., Liu, Y.S., Chen, X.D., Wang, J., Shi, Z.H., Chen, F.Q., Zha, D.J., Xue, T., 2021. Nrg1/ErbB2 regulates differentiation and apoptosis of neural stem cells in the cochlear nucleus through PI3K/Akt pathway. Neurosci. Lett. 751, 135803.
Marlowe, C., Clark, M.J., Mast, R.W., Friedman, M.A., Waddell, W.J., 1986. The distribution of [14C]acrylamide in male and pregnant Swiss-Webster mice studied by whole-body autoradiography. Toxicol. Appl. Pharmacol. 86 (3), 457–465.
Martini, S., Bernoth, K., Main, H., Ortega, G.D., Lendahl, U., Just, U., Schwanbeck, R., 2013. A critical role for Sox9 in notch-induced astrogliogenesis and stem cell maintenance. Stem Cells 31 (4), 741–751.
Nagai, J., Rajbhandari, A.K., Gangwani, M.R., Hachisuka, A., Coppola, G., Masmanidis, S. C., Fanselow, M.S., Khakh, B.S., 2019. Hyperactivity with disrupted attention by activation of an astrocyte synaptogenic cue. Cell 177 (5), 1280–1292 e1220.
Numakawa, T., Suzuki, S., Kumamaru, E., Adachi, N., Richards, M., Kunugi, H., 2010. BDNF function and intracellular signaling in neurons. Histol. Histopathol. 25 (2), 237–258.
Ogawa, B., Ohishi, T., Wang, L., Takahashi, M., Taniai, E., Hayashi, H., Mitsumori, K., Shibutani, M., 2011. Disruptive neuronal development by acrylamide in the hippocampal dentate hilus after developmental exposure in rats. Arch. Toxicol. 85 (8), 987–994.
Ogawa, B., Wang, L., Ohishi, T., Taniai, E., Akane, H., Suzuki, K., Mitsumori, K., Shibutani, M., 2012. Reversible aberration of neurogenesis targeting late-stage progenitor cells in the hippocampal dentate gyrus of rat offspring after maternal exposure to acrylamide. Arch. Toxicol. 86 (5), 779–790.
Pabst, K., Mathar, W., Palavinskas, R., Meisel, H., Blüthgen, A., Klaffke, H., 2005. Acrylamide-occurrence in mixed concentrate feed for dairy cows and carry-over into milk. Food Addit. Contam. 22 (3), 210–213.
Park, H.R., Kim, M.S., Kim, S.J., Park, M., Kong, K.H., Kim, H.S., Kwack, S.J., Kang, T.S., Kim, S.H., Kim, H.S., Lee, J., 2010. Acrylamide induces cell death in neural progenitor cells and impairs hippocampal neurogenesis. Toxicol. Lett. 193 (1), 86–93.
Park, K., Lee, S.J., 2020. Deciphering the star codings: astrocyte manipulation alters mouse behavior. Exp. Mol. Med. 52 (7), 1028–1038.
Patterson, S.L., Abel, T., Deuel, T.A., Martin, K.C., Rose, J.C., Kandel, E.R., 1996. Recombinant BDNF rescues deficits in basal synaptic transmission and hippocampal LTP in BDNF knockout mice. Neuron 16 (6), 1137–1145.

Pedersen, M., von Stedingk, H., Botsivali, M., Agramunt, S., Alexander, J., Brunborg, G., Chatzi, L., Fleming, S., Fthenou, E., Granum, B., Gutzkow, K.B., Hardie, L.J., Knudsen, L.E., Kyrtopoulos, S.A., Mendez, M.A., Merlo, D.F., Nielsen, J.K., Rydberg, P., Segerbäck, D., Sunyer, J., Wright, J., Törnqvist, M., Kleinjans, J.C., Kogevinas, M., 2012. Birth weight, head circumference, and prenatal exposure to acrylamide from maternal diet: the European prospective mother-child study (NewGeneris). Environ. Health Perspect. 120 (12), 1739–1745.

Pedersen, M., Vryonidis, E., Joensen, A., Törnqvist, M., 2022. Hemoglobin adducts of acrylamide in human blood - what has been done and what is next? Food Chem. Toxicol. 161, 112799.

de Pins, B., Cifuentes-Díaz, C., Farah, A.T., López-Molina, L., Montalban, E., Sancho-Balsells, A., López, A., Ginés, S., Delgado-García, J.M., Alberch, J., Gruart, A., Girault, J.A., Giralt, A., 2019. Conditional BDNF delivery from astrocytes rescues memory deficits, spine density, and synaptic properties in the 5xFAD mouse model of Alzheimer disease. J. Neurosci. 39 (13), 2441–2458.

Pistollato, F., Louisse, J., Scelfo, B., Mennecozzi, M., Accordi, B., Basso, G., Gaspar, J.A., Zagoura, D., Barilari, M., Palosaari, T., Sachinidis, A., Bremer-Hoffmann, S., 2014. Development of a pluripotent stem cell derived neuronal model to identify chemically induced pathway perturbations in relation to neurotoxicity: effects of CREB pathway inhibition. Toxicol. Appl. Pharmacol. 280 (2), 378–388.

Pistollato, F., Canovas-Jorda, D., Zagoura, D., Bal-Price, A., 2017a. Nrf2 pathway activation upon rotenone treatment in human iPSC-derived neural stem cells undergoing differentiation towards neurons and astrocytes. Neurochem. Int. 108, 457–471.

Pistollato, F., Canovas-Jorda, D., Zagoura, D., Price, A., 2017b. Protocol for the differentiation of human induced pluripotent stem cells into mixed cultures of neurons and glia for neurotoxicity testing. J. Vis. Exp. (124).

Pistollato, F., de Gyves, E.M., Carpi, D., Bopp, S.K., Nunes, C., Worth, A., Bal-Price, A., 2020. Assessment of developmental neurotoxicity induced by chemical mixtures using an adverse outcome pathway concept. Environ. Health 19 (1), 23.

Pistollato, F., Carpi, D., Mendoza-de Gyves, E., Paini, A., Bopp, S.K., Worth, A., Bal-Price, A., 2021. Combining in vitro assays and mathematical modelling to study developmental neurotoxicity induced by chemical mixtures. Reprod. Toxicol. 105, 101–119.

Poo, M.M., 2001. Neurotrophins as synaptic modulators. Nat. Rev. Neurosci. 2 (1), 24–32.

Radad, K., Al-Shraim, M., Al-Emam, A., Moldzio, R., Rausch, W.D., 2019. Neurotoxic effects of acrylamide on dopaminergic neurons in primary mesencephalic cell culture. Folia Neuropathol. 57 (2), 196–204.

Rice, D., Barone Jr., S., 2000. Critical periods of vulnerability for the developing nervous system: evidence from humans and animal models. Environ. Health Perspect. 108 (Suppl. 3), S511–S533.

RStatisticalProject, 2022. ⟨https://www.r-project.org/⟩. (Accessed 10 April 2022).

Sachana, M., Rolaki, A., Bal-Price, A., 2018. Development of the adverse outcome pathway (AOP): chronic binding of antagonist to N-methyl-d-aspartate receptors (NMDARs) during brain development induces impairment of learning and memory abilities of children. Toxicol. Appl. Pharmacol. 354, 153–175.

Sachana, M., Shafer, T.J., Terron, A., 2021. Toward a better testing paradigm for developmental neurotoxicity: OECD efforts and regulatory considerations. Biology 10 (2).

Saha, R.N., Liu, X., Pahan, K., 2006. Up-regulation of BDNF in astrocytes by TNF-alpha: a case for the neuroprotective role of cytokine. J. Neuroimmune Pharmacol. 1 (3), 212–222.

Schmittgen, T.D., Livak, K.J., 2008. Analyzing real-time PCR data by the comparative C (T) method. Nat. Protoc. 3 (6), 1101–1108.

Schmuck, M.R., Temme, T., Dach, K., de Boer, D., Barenys, M., Bendt, F., Mosig, A., Fritsche, E., 2017. Omnisphero: a high-content image analysis (HCA) approach for phenotypic developmental neurotoxicity (DNT) screenings of organoid neurosphere cultures in vitro. Arch. Toxicol. 91 (4), 2017–2028.

Settels, E., Bernauer, U., Palavinskas, R., Klaffke, H.S., Gundert-Remy, U., Appel, K.E., 2008. Human CYP2E1 mediates the formation of glycidamide from acrylamide. Arch. Toxicol. 82 (10), 717–727.

Silbereis, J.C., Pochareddy, S., Zhu, Y., Li, M., Sestan, N., 2016. The cellular and molecular landscapes of the developing human central nervous system. Neuron 89 (2), 248–268.

Smith, E.A., Oehme, F.W., 1991. Acrylamide and polyacrylamide: a review of production, use, environmental fate and neurotoxicity. Rev. Environ. Health 9 (4), 215–228.

Sörgel, F., Weissenbacher, R., Kinzig-Schippers, M., Hofmann, A., Illauer, M., Skott, A., Landersdorfer, C., 2002. Acrylamide: increased concentrations in homemade food and first evidence of its variable absorption from food, variable metabolism and placental and breast milk transfer in humans. Chemotherapy 48 (6), 267–274.

Spinu, N., Bal-Price, A., Cronin, M.T.D., Enoch, S.J., Madden, J.C., Worth, A.P., 2019. Development and analysis of an adverse outcome pathway network for human neurotoxicity. Arch. Toxicol. 93 (10), 2759–2772.

Stansfield, K.H., Pilsner, J.R., Lu, Q., Wright, R.O., Guilarte, T.R., 2012. Dysregulation of BDNF-TrkB signaling in developing hippocampal neurons by Pb(2+): implications for an environmental basis of neurodevelopmental disorders. Toxicol. Sci. 127 (1), 277–295.

von Stedingk, H., Vikström, A.C., Rydberg, P., Pedersen, M., Nielsen, J.K., Segerbäck, D., Knudsen, L.E., Törnqvist, M., 2011. Analysis of hemoglobin adducts from acrylamide, glycidamide, and ethylene oxide in paired mother/cord blood samples from Denmark. Chem. Res. Toxicol. 24 (11), 1957–1965.

Stiles, J., Jernigan, T.L., 2010. The basics of brain development. Neuropsychol. Rev. 20 (4), 327–348.

Stolt, C.C., Lommes, P., Sock, E., Chaboissier, M.C., Schedl, A., Wegner, M., 2003. The Sox9 transcription factor determines glial fate choice in the developing spinal cord. Genes Dev. 17 (13), 1677–1689.

Sumner, S.C., Williams, C.C., Snyder, R.W., Krol, W.L., Asgharian, B., Fennell, T.R., 2003. Acrylamide: a comparison of metabolism and hemoglobin adducts in rodents following dermal, intraperitoneal, oral, or inhalation exposure. Toxicol. Sci. 75 (2), 260–270.

Tareke, E., Rydberg, P., Karlsson, P., Eriksson, S., Törnqvist, M., 2002. Analysis of acrylamide, a carcinogen formed in heated foodstuffs. J. Agric. Food Chem. 50 (17), 4998–5006.

ThermoFisherScientific, 2022. ⟨https://www.thermofisher.com/no/en/home/life-science/cell-analysis/cellular-imaging/hcs-hca/sample-data.html⟩. (Accessed 10 April 2022).

Tilson, H.A., 1981. The neurotoxicity of acrylamide: an overview. Neurobehav. Toxicol. Teratol. 3 (4), 445–461.

van Thriel, C., Westerink, R.H., Beste, C., Bale, A.S., Lein, P.J., Leist, M., 2012. Translating neurobehavioural endpoints of developmental neurotoxicity tests into in vitro assays and readouts. Neurotoxicology 33 (4), 911–924.

Venkatesh, K., Srikanth, L., Vengamma, B., Chandrasekhar, C., Prasad, B.C., Sarma, P.V., 2015. In vitro transdifferentiation of human cultured CD34+ stem cells into oligodendrocyte precursors using thyroid hormones. Neurosci. Lett. 588, 36–41.

Vikstrom, A.C., Abramsson-Zetterberg, L., Naruszewicz, M., Athanassiadis, I., Granath, F. N., Tornqvist, M.A., 2011. In vivo doses of acrylamide and glycidamide in humans after intake of acrylamide-rich food. Toxicol. Sci. 119 (1), 41–49.

Wise, L.D., Gordon, L.R., Soper, K.A., Duchai, D.M., Morrissey, R.E., 1995. Developmental neurotoxicity evaluation of acrylamide in Sprague-Dawley rats. Neurotoxicol. Teratol. 17 (2), 189–198.

Young, J.F., Luecke, R.H., Doerge, D.R., 2007. Physiologically based pharmacokinetic/pharmacodynamic model for acrylamide and its metabolites in mice, rats, and humans. Chem. Res. Toxicol. 20 (3), 388–399.

Zagoura, D., Canovas-Jorda, D., Pistollato, F., Bremer-Hoffmann, S., Bal-Price, A., 2017. Evaluation of the rotenone-induced activation of the Nrf2 pathway in a neuronal model derived from human induced pluripotent stem cells. Neurochem. Int. 106, 62–73.

Zhou, Y., Zhou, B., Pache, L., Chang, M., Khodabakhshi, A.H., Tanaseichuk, O., Benner, C., Chanda, S.K., 2019. Metascape provides a biologist-oriented resource for the analysis of systems-level datasets. Nat. Commun. 10 (1), 1523.